A practical introduction to quantum scattering theory, and beyond

Calvin W. Johnson

June 29, 2017

Contents

Introduction

I will tell you up front: I am not an expert in scattering theory. My own background is in many-body theory which deals with bound states; an astute reader might on her own detect that predilection in what follows. Yet we interact with bound state systems through elastic and inelastic scattering and through reactions. Therefore I wrote this book largely to teach myself and my students how to calculate scattering and capture rates. Because of that, I emphasize practical, numerical calculations, starting with simple analytic systems such as a square well potential, but later discussing in detail how to actually carry out nontrivial calculations. I do not provide sample codes, in part because different readers will favor different tools (Mathematica/MatLab, Python, or C or Fortran–I tend to use Fortran), and in part because I think you will learn this best by writing your own code. But I will provide results you can compare your codes against. This book will not exhaust the field of scattering. It focuses on parameterizing the S-matrix through phase shifts in channels of good angular momentum, the so-called partial-wave decomposition. I spend a great deal of time on how to calculate phase shifts in various ways, including and especially in the J-matrix formalism, which uses a bound state basis. But I leave out or only briefly discuss the optical theorem, the Born approximation, form factors, and the eikonal approximation.

I heavily rely upon examples, in particular the finite square well potential, which can be solved analytically, but which also makes a suitable target for simple numerical calculations. I encourage readers to attempt to replicate in detail these examples.

This book assumes the reader has had quantum mechanics at the level of at least Griffiths or Shankar, learning the formal Dirac bra-ket notation, the Schrödinger equation in three-dimensions especially in spherical coordinates, including the hydrogen atom. This book also assumes the reader has good skill in some computational platform, although it could be easily combined with a course in computational methods. If you do not have strong computational skills, a more formal text in scattering may be better for you.

While scattering theory is a common topics, I chose to write this book because most quantum mechanics texts give only a brief introduction, and most books on scattering theory emphasis formal mathematics over practical calculations.

Part I

The basics of quantum scattering

Chapter 1

Cross-sections: a window on the microscopic world

How do we see the tiniest of things? The wavelength of visible light is a few hundred nanometers (10^{-9} m), which is thousands of times larger than atoms. The wavelength of high energy gamma rays are tens of femtometers (10^{-15} m), which is also larger than individual nuclei. These objects cannot be photographed; there is no microscope through which we can peer and see them wriggling on the slide.

The answer came from Rutherford's groundbreaking 1911 [?? gotta check] experiment. These were heady times, and it is hard for us today to conceive of how swiftly our conception of nature was changing. In 1899 J.J. Thompson had discovered the electron, the carrier of electric current. Electrons are part of atoms, but even the reality of atoms themselves, those un-cuttable objects postulated more than two millenia before by the Greek philosopher Democritus, only became widely accepted after Einstein's 1905 Ph.D thesis demonstrated the connection between Brownian motion and the atomic hypothesis. Because electrons were negatively charged (an assignment due to an unlucky guess by Benjamin Franklin) and atoms neutral, atoms had to have a positively charged component. British physicists postulated a "plum pudding" model, a description singularly unhelpful to anyone unfamiliar with English desserts, in which the electrons were embedded in a positively charged matrix.

Rutherford drilled a hole in a block of lead and placed inside it a bit of polonium, one of the new elements recently discovered by the indefatigable Marie Curie. Polonium was known to emit alpha rays, bits of positively charged matter but much heavier than electrons; this was easy to establish, because by putting in a magnetic field you could measure the ratio of mass to charge. Thus out of the block of lead came a narrow–the technical term is *collimated*–beam of alpha particles.

This alpha beam Rutherford aimed at a thin sheet of gold foil. Rutherford wanted to know how the alpha rays were deflected by the gold atoms, so all

around the gold foil he set a phosphorescent screen. When an alpha particle struck the screen, it would be announced by a flash of light.

Rutherford, or more accurately, his assistants Geiger and Marsden, then meticulously counted the rate at which alpha particles were deflected at different angles. Today we have fast electronic assistants to do this kind of things, but back them Geiger or Marsden would take turns staring through an eyepiece at a section of phosphorescent screen of fixed area, calling out flashes, while the other noted the counts and kept an eye on the clock. (This story is better told, and in more details, in Cathcart's book *The Fly in the Cathedral*, which I highly recommend.)

Plotted as count rate versus angle, they found the experimental curve was neatly described as proportional to $1/\sin^4(\theta/2)$, where θ is the scattering angle. That particular formulation was not empirical, but exactly what one could expect if the positively charged alpha particles were scattering off another positively charged object, but of infinitesmal radius. Rutherford knew the rough size of atoms, which Thompson scattering tells us, but the data showed that whatever the alpha particles were scattering off, it was far, far smaller. Today we know the nucleus of the atom, composed of protons and neutrons (which were not discovered until 1932 by James Chadwick), is around 100,000 times smaller than the cloud of electrons swarming around it.

So this is how we see the microscopic–or better, the sub-microscopic–world: we take little things we cannot see, but we can count, and throw them at other little things we cannot see, and we see how they scatter.

Furthermore, we characterize our answers in terms of the *cross-section*, which has units of area, and which is very much "how big" the target appears to be. By looking at a little more detail at the Rutherford-Geiger-Marsden experiment, we can foreshadow some key points. In particular:

Our standard conceptual setup of an experiment has two components and three regions. The components are the *target*, such as the gold atoms, and the *projectile*, such as the alpha particles. While the target is fixed–later we will worry about frame of reference–the projectile passes through three distinct regions. In the beginning it is *incoming* as a uniform collimated beam. Classically you can think of this as beam of particles all with the same momentum vectors; quantum mechanically we call this a *plane wave*. We quantify the incoming beam by its *flux*, which is the number of particles passing through a unit area per unit time. In essence, we imagine a little window in space and count how many particles pass through it. The particle, or at least some of them, reach the target, or the *interaction region*.

Any *outgoing* particle that is scattered now has a new momentum vector pointing back to the target; the scattered particles do not have the same or even parallel momentum vectors. The way we measure scattering is to again, have a window at some distance from the target and count the particles passing through it, as when Geiger and Marsden pressed their eyes to their viewing scopes. There is an important difference, however. For the incoming flux, became the momenta were parallel, we could in principle measure anywhere

along the beam. But now that the particles are scattering out from a pointlike target, the actual count through an area falls off with the inverse of the distance squared. But we are now measuring with angles, so we want the count through a solid angle.

[Eventually I'll add figures to help illustrate this.]

Experimentally, what we measure as the physically meaningful quantity is

rate of outgoing particles through a solid angle
over
rate of incoming particles through an area

This ratio has units of area, and we call it the *cross-section*. As befits the origin story of scattering, with Geiger and Marsden trading turns staring at a little patch of phosphorescent screen, it has become our window on the submicroscopic world.

Also befitting the origins of scattering is the main unit of cross-sections. Historically, in the century after Newton's invention of calculus mathematical physics was largely taken over by French mathematicians, hence the preponderance of French names: Laguerre, Legendre, and Hermite polynomials are the daily diet of junior physicists struggling to solve differential equations. Quantum mechanics was dominated by German physicists, hence *eigen*states and *Ansätze*. But in the years between the world wars, English-speaking experimental physicists, began, if not to dominate, then to make significant contributions, and in the U.S. in particular these often came from rural or working-class backgrounds. Hence the colloquial origin of a term probably as puzzling to non-English speakers as "plum pudding" is to anyone outside the British Commonwealth: the *barn*, as in the phase, *couldn't hit the broad side of a barn.* A *barn* is 10^{-24} cm^2.

1.1 Adding quantum mechanics: current, flux, and the scattering amplitude

I've introduced a fundamental idea, which is that we learn about a tiny object by measuring the ratio of *particles out* to *particles in*, and that this ratio has units of *area* and is called the *cross section*. Now we want to start to develop a theory of this scattering, and because the target is very, very tiny, we invoke the theory of tiny things, or, more formally, of tiny *action*: quantum mechanics.

The wave function for *incoming* particles is easy. We assume a beam of particles with uniform momentum $\vec{p}$, and in quantum mechanics the momentum operator in coordinate space is $\frac{\hbar}{i}\vec{\nabla}$. An eigenstate of this operator is a *plane wave*, $\exp(i\vec{p}\cdot\vec{r}/\hbar)$.

Normalization of any wave function is crucial in quantum mechanics. While I discuss this in detail in section 4.1, for now let's assume we put our plane wave in a cubic box with each side of length L, so that the volume is L^3. Of course, this ignores the important issue of boundary conditions, so we don't really have

a true plane wave, but being physicists we set aside that unpleasantness until later. Then the normalized, sort-of plane wave in a cube L^3 is

$$\frac{1}{L^{3/2}} \exp\left(i\frac{\vec{p}\cdot\vec{r}}{\hbar}\right). \tag{1.1}$$

Now let's look at another idea, which is not always emphasized in introductory quantum texts but which will be fundamental for us: the quantum *current*. Here is a brief reminder of the standard motivation: for any time-dependent wave function $\Psi(\vec{r},t)$, the probability *density* is of course $\rho(\vec{r},t) = \Psi(\vec{r},t)^*\Psi(\vec{r},t)$. If we do not have a stationary state, that is, if we cannot factorize $\Psi(\vec{r},t) = \psi(\vec{r})\exp(-iEt/\hbar)$–and although in introductory courses that kind of factorization is often assumed, the most general solutions to the time-dependent Schrödinger equation cannot be so factorized–then $\rho(\vec{r},t)$ can change in time. We then invoke an idea from classical fluid flow, that is the *continuity equation*,

$$\frac{\partial\rho(\vec{r},t)}{\partial t} + \vec{\nabla}\cdot\vec{J}(\vec{r},t) = 0, \tag{1.2}$$

where $\vec{J}(\vec{r},t)$ is the *current*. Most introductory quantum texts show that

$$\vec{J} = \frac{\hbar}{2Mi}\left(\Psi^*\vec{\nabla}\Psi - \Psi\vec{\nabla}\Psi^*\right). \tag{1.3}$$

For a plane wave (1.1) with momentum $\vec{p}$, the current is

$$\vec{J}_{\text{plane wave}} = \frac{\vec{p}}{M}\frac{1}{\text{Vol}} = \frac{\hbar\vec{k}}{M}\frac{1}{\text{Vol}}. \tag{1.4}$$

Here I've introduce the *wave vector* $\vec{k} = \vec{p}/\hbar$, whose magnitude k is called the *wave number*, which has dimensions of 1/length; many of our results will be stated in terms of the wave number.

Note that the current for a plane wave in a box, (1.4) has exactly units of time^{-1} area^1, that is, we can interpret it as a *flux*. This will be very important to us later!

So much for the incoming particles. What about the outgoing particles? Because the particles are scattered off a target that is, macroscopically, a point, we can no longer talk about plane waves, but rather spherical waves. An *outgoing spherical wave* is

$$\frac{\exp(ikr)}{r}, \tag{1.5}$$

a result I'll later justify using Green's functions (chapter to be written). Because we want/know our final result to depend upon the scattering angle, we further write

$$\psi_{\text{out}} = f(\theta)\frac{\exp(ikr)}{r}, \tag{1.6}$$

where $f(\theta)$ is the *scattering amplitude*. Here we have not normalized to a box, or else absorbed it into the definition of f. To find the flux for this outgoing

wave, remember that in spherical coordinates the gradient is

$$\vec{\nabla} = \hat{e}_r \frac{\partial}{\partial r} + \hat{e}_\theta \frac{1}{r}\frac{\partial}{\partial \theta} + \hat{e}_\phi \frac{1}{r\sin\theta}\frac{\partial}{\partial \phi} \tag{1.7}$$

so that

$$\vec{\nabla}\psi_{\text{out}} = ik\hat{e}_r\psi_{\text{out}} + \mathcal{O}\left(\frac{1}{r}\right)\psi_{\text{out}}, \tag{1.8}$$

and as $r \to \infty$ only the first term survives. Then the current for ψ_{out} is

$$\vec{J}_{\text{out}} \underset{r\to\infty}{\to} \frac{\hbar k}{M}\frac{\hat{e}_r}{r^2}|f(\theta)|^2. \tag{1.9}$$

When this scatters at an angle θ the amount of flux through a solid angle $\Delta\Omega$ at a distance r, and thus through an area Ωr^2, is

$$\frac{\hbar k}{M}|f(\theta)|^2\Delta\Omega.$$

Now let's put these together. Dropping the normalization to a box of volume L^3, we consider the full scattering wavefunction, with both incoming and outgoing pieces, Ψ_{scatt}. We can only "measure" the wave function at a "large" distance r from the target, which means

$$\Psi_{\text{scatter}} \underset{r\to\infty}{\to} e^{i\vec{k}\cdot\vec{r}} + f(\theta)\frac{\exp(ikr)}{r}. \tag{1.10}$$

The cross section is just the ratio, of the incoming and outgoing, that is,

$$\frac{d\sigma}{d\theta} = |f(\theta)|^2. \tag{1.11}$$

Hence, in much of what we will do in this book is to find ways to characterize and numerically calculate the scattering amplitude f, and thus the cross-section σ, through concepts such as *phase shifts*, the S-matrix, and others.

1.2 Other matters, maybe

Including a brief discussion of the Born approximation, Rutherford scattering, and form factors.

1.3 Project 1

At the end of each chapter I will propose for you a project to help you pull together your knowledge and skills.

For this chapter, I want you to hunt down *experimental* cross-sections in your field. Despite its heavy reliance upon theory and rigorous mathematics, like all science physics is ultimately and always empirical, and the best way to become skilled in the topic is to have a store of knowledge of experimental results.

Chapter 2

Phase shifts and the partial wave decomposition

One way to characterize or parameterize cross-sections σ or the scattering amplitude $f(\theta)$, which I introduced in the first chapter, is through *phase shifts*. Phase shifts start with the idea that, far away from the interaction region, that is, where the projectile interacts with the target or, more formally, where the interaction potential vanishes, the particle is free. For particles with zero relative angular momentum, that is, with orbital angular momentum $\ell = 0$ (also called an s-wave), this looks like some combination of sines and cosines, that is, simple waves. As discussed in the next section, if there were no scattering potential, the solution would be a pure sine wave everywhere. If we add a scattering potential, however, beyond the range of the potential the particle is still free, but the phase of the wavefunction is now shifted: hence the name.

Most texts derive phase shifts from the so-called *partial wave decomposition* or expansion, where one takes solutions to the Schrödinger equation and decompose it into part of good orbital angular momentum. We will do so below in section 2.3, but we will first simply explore the idea of a phase shift before carrying out this somewhat complicated derivation.

2.1 What is a phase shift?

The basic idea is that scattering is localized, so that at some distance the scattering particle is free. The radial Schrödinger equation a particle of mass mc is

$$-\frac{\hbar^2}{2m}\frac{d^2}{dr^2}u(r) + \frac{\hbar^2\ell(\ell+1)}{2mr^2}u(r) + V(r)u(r) = Eu(r) \tag{2.1}$$

where ℓ is the orbital angular momentum. First, let's think about the case with $\ell = 0$, that is, s-wave scattering. For a free particle, $V = 0$, the solutions are

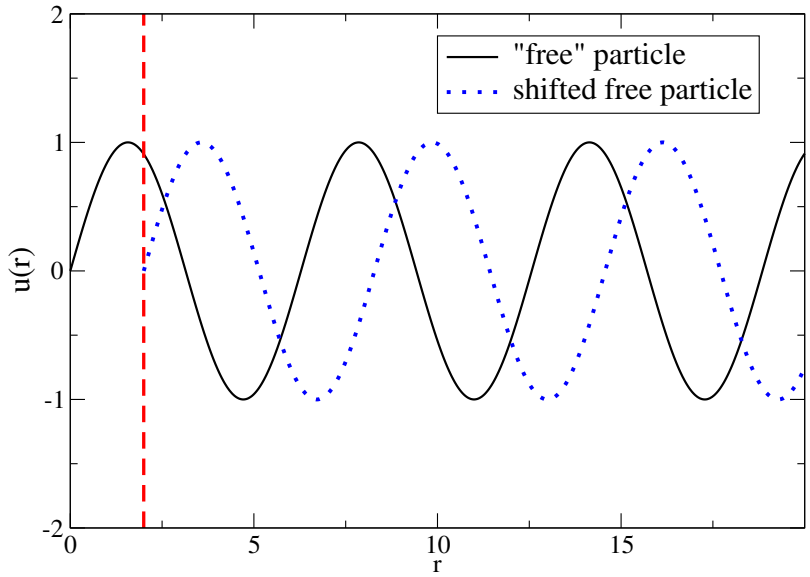

Figure 2.1: Illustration of the shift in s-wave ($\ell = 0$) wave function due to a hard sphere at $r = 2$ (dashed red vertical line). Solid black line is the "free" particle wave function, while the blue dotted line is for the particle in the presence of the hard sphere.

linear combinations of sine and cosine functions, that is,

$$u(r) = A\sin(kr) + B\cos(kr), \tag{2.2}$$

where $k = p/\hbar = \sqrt{2mE}/\hbar$ is the wavenumber. Now if the potential vanishes everywhere, the only boundary condition is at the origin and $u(0) = 0$ and we are restricted to sine functions, that is, $B = 0$.

But now suppose $V(r) \neq 0$ for r within some radial distance R. For $r > 0$ we stil have a free particle, but we no longer have the boundary condition. Therefore we can have $B \neq 0$. More generally we write

$$u(r) = C\sin(kr + \delta), \tag{2.3}$$

where by trigonometric identities $A = C\cos\delta$, $B = C\sin\delta$, and finally $\tan\delta = B/A$. We'll see later that the phase shift δ is a function of the wavenumber k, which mean it depends upon the momentum p or the energy E.

Example: the hard sphere. As a simple example, consider the *hard sphere*, where $V = \infty$ for $r \leq R$. This means we have a boundary condition $u(R) = 0$ or $\sin(kR + \delta) = 0$; hence $\delta(k) = -kR$. This is shown in Fig. 2.1 for a particle with orbtial angular momentum $\ell = 0$ (or s-wave). The "free" particle is just a sine function, with the boundary condition $u(0) = 0$, here seen as the black solid line. The blue dotted line shows the shift in the free particle wave

function, which now has a boundary condition at $u(R) = 0$. In this example $R = 2$. This is a key example of phase shifts, and all other cases are just more complicated cases of this.

What about for $\ell > 0$? Then the free particle solutions are *spherical Bessel* and *spherical Neumann* functions:

$$u_\ell(r) = A_\ell\, r j_\ell(kr) - B_\ell\, r n_\ell(kr). \tag{2.4}$$

The basic properties of spherical Bessel functions, including how to numerically generate them, can be found in section C.1 of the appendices. For now, just know that

$$j_\ell(x) \underset{x\to\infty}{\to} \frac{\sin\left(x - \ell\frac{\pi}{2}\right)}{x}, \tag{2.5}$$

$$n_\ell(x) \underset{x\to\infty}{\to} -\frac{\cos\left(x - \ell\frac{\pi}{2}\right)}{x}. \tag{2.6}$$

The minus sign in front of the limit of the spherical Neumann function explains the difference in sign between (2.4) and (2.2). From this we can generalize phase shifts for any value of ℓ:

$$u_\ell(r) = r j_\ell\left(kr - \ell\frac{\pi}{2} + \delta_\ell(k)\right), \tag{2.7}$$

where

$$\tan\delta_\ell = \frac{B_\ell}{A_\ell}. \tag{2.8}$$

Example: the hard sphere redux Consider again the hard sphere but for arbitrary ℓ. We have the boundary condition

$$u_\ell(R) = A_\ell\, R j_\ell(kR) - B_\ell\, R n_\ell(kR) = 0, \tag{2.9}$$

or

$$\tan\delta_\ell(k) = \frac{B_\ell}{A_\ell} = \frac{j_\ell(kR)}{n_\ell(kR)}. \tag{2.10}$$

2.2 Scattering off a finite square well potential

We will be using the finite square well of depth $-V_0$ and radius R, that is,

$$V(r) = \begin{cases} -V_0, & r \le R, \\ 0, & r > R \end{cases} \tag{2.11}$$

over and over; we will solve it analytically, but then use it as a test case for numerical calculations.

First, let's do it for s-wave scattering, or $\ell = 0$. This is easier to visualize. To solve the finite square well, we divide and conquer two regions: region 1 is for $0 \le r \le R$, and region 2 is for $R \le r \le \infty$; the radial wavefunctions $u_{1,2}(r)$

and their first derivatives must match at $r = R$. In both cases the solutions are sine functions; in region 1, with a boundary condition $u_1(0) = 0$, it is

$$u_1(r) = A \sin Kr,$$

where $E = \hbar^2 K^2/2m + V_0$, that is,

$$K = \frac{\sqrt{2m(E + V_0)}}{\hbar}$$

and in region 2, we can either take sine and cosine functions, or, more directly, a sine function with a shift phase:

$$u_2(r) = \sin(kr + \delta),$$

where $k = \sqrt{2mE}/\hbar$. You will note I did not put a normalization constant on u_2. For now we only need the relative normalization between u_1 and u_2; the absolute normalization for scattering states we put off until section 4.1.

To find the phase shift δ, we need to match at $r = R$ both the wavefunctions, $u_1(R) = u_2(R)$,

$$A \sin KR = \sin(kR + \delta), \tag{2.12}$$

and their first derivatives, $u_1'(R) = u_2'(R)$,

$$AK \cos KR = k \cos(kR + \delta). \tag{2.13}$$

Finally we divide (2.12) by (2.13) to eliminate the constant A and get

$$k \tan KR = K \tan(kR + \delta).$$

Solving, we find

$$\delta = -kR + \tan^{-1}\left(\frac{k}{K} \tan KR\right) \tag{2.14}$$

We can simplify this a bit by introducing $K_0 = \sqrt{2mV_0}/\hbar$, so that $K = \sqrt{K_0^2 + k^2}$. We'll use this later.

Fig. 2.2 shows the $\ell = 0$ phase shift for a square well with $m = \hbar = 1$ and for a radius $R = 1$, for various depths V_0. Note that at $V_0 = 1$ the phase shift rises sharply, while at $V_0 = 1$ it starts off negative. As we'll discuss later, what has happens is as V_0 increases, a bound state appears.

The apparent discontinuity in the phase shift for $V_0 = 1.5$ is really just an ambiguity in angle: here δ is restricted to be between $-\pi$ and $+\pi$ radians. Because of this ambiguity, it is sometimes convenient to plot $k \cot \delta_0$, shows in Fig.2.3 . Shortly we will see that we can interpret the y-intercept and slope of $k \cot \delta$ in terms of fundamental quantities called the *scattering length* and *effective range*. Again, as the y-intercept passes through zero, we will see this corresponds to a bound state.

Notice in Fig. 2.2 that as one increases V_0, the phase shift is initially positive, but with increasing slope. As one goes from $V_0 = 1$ to $V_0 = 1.5$, however the

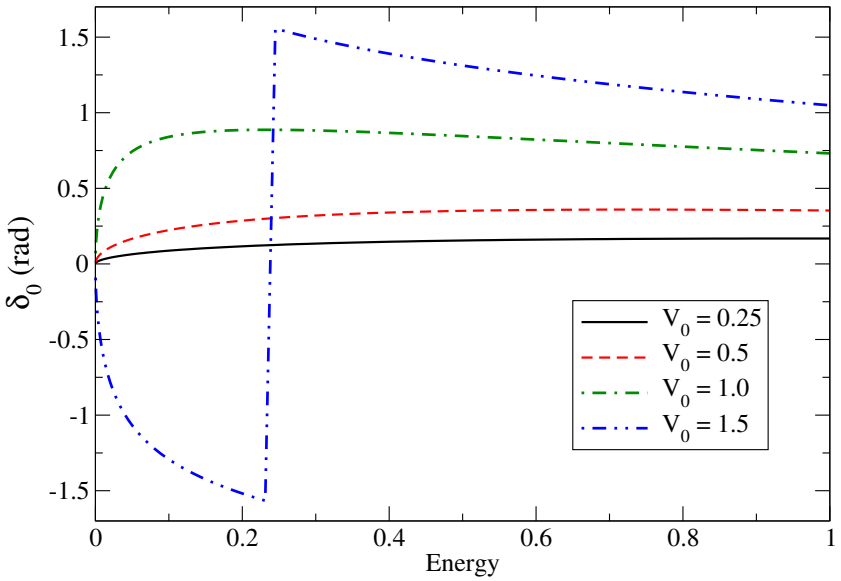

Figure 2.2: $\ell = 0$ phase shift δ_0 (in radians) for a square well with $m = \hbar = R = 1$ for several depths V_0, versus energy $= \hbar^2 k^2/2m$.

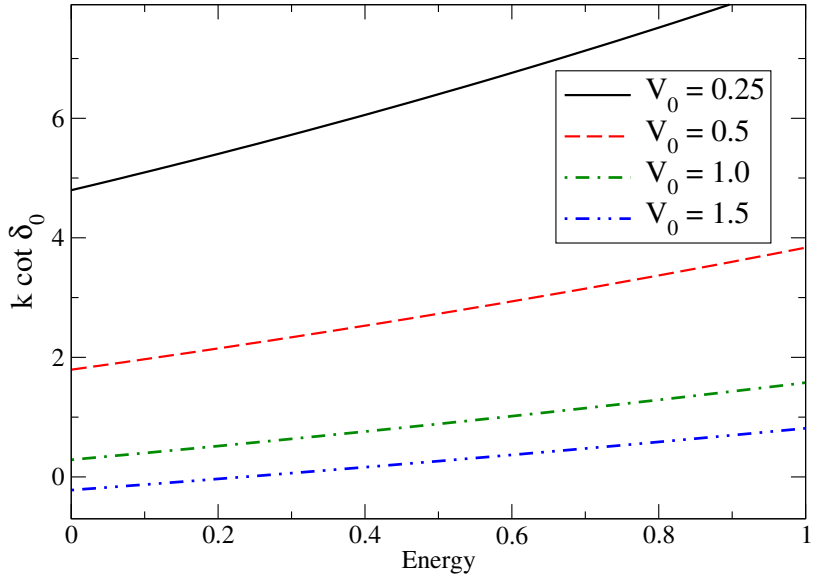

Figure 2.3: $k \cot \delta_0$ for a square well with $m = \hbar = R = 1$ for several depths V_0, versus energy $= \hbar^2 k^2/2m$.

phase shift become negative. At the same time one sees the y-intercept in Fig. 2.3 pass through zero from positive to negative. Later, when we discuss *Levinson's theorem*, we will see both of these are associated with a new bound state appearing as V_0 is increased (also see Fig. 4.2).

Exercise 2.1: Using any numerical platform you like (Python, MatLab, Mathematica, C/C++, Fortran...) reproduce Figs. 2.2 and 2.3. Go futher and increase the depth. Does the y-intercept of $k \cot \delta_0$ become positive again?

Exercise 2.2: *Square well with a hard core.* Consider a potential with a hard core out to some R_c, and an attractive square well of depth V_0 from $R_c < r \leq R$. Find the $\ell = 0$ phase shifts analytically.

We can also generalize to angular momenta with $\ell > 0$, where the general 'free particle' solution is (2.4). For $u_1(r)$, we have the boundary condition $u_1(0) = 0$, which only the spherical bessel function j_ℓ satisfies:

$$u_1(r) = r j_\ell(Kr) \tag{2.15}$$

while for $r \geq R$ we have the general solution

$$u_2(r) = A_\ell r j_\ell(kr) - B_\ell r n_\ell(kr). \tag{2.16}$$

Again we match the wavefunctions at the boundary,

$$R j_\ell(KR) = A_\ell R j_\ell(kR) - B_\ell R n_\ell(kR).$$

The overall factor of R of course cancels out. We also need to match derivatives across the boundary. For that we need (C.8), e.g.,

$$\frac{d}{dr}\left(r j_\ell(kr)\right) = \frac{d}{d(kr)}\left(kr j_\ell(kr)\right) = k\left(-r j_{\ell+1}(kr) + \frac{\ell+1}{kr} r j_\ell(kr)\right)$$

and similarly for the Neumann function, and after cancelling R from both sides, obtain

$$K\left(-j_{\ell+1}(KR) + \frac{\ell+1}{KR} j_\ell(KR)\right)$$
$$= k\left[A_\ell\left(-j_{\ell+1}(kR) + \frac{\ell+1}{kR} j_\ell(kR)\right) - B_\ell\left(-n_{\ell+1}(kR) + \frac{\ell+1}{kR} n_\ell(kR)\right)\right]$$

To get the phase shift, we need (2.8), let's first solve for B_ℓ:

$$B_\ell = \left(A_\ell j_\ell(kR) - j_\ell(KR)\right)/n_\ell(kR)$$

so that

$$\tan \delta_\ell = \frac{B_\ell}{A_\ell} = \frac{j_\ell(kR)}{n_\ell(kR)} - \frac{j_\ell(KR)}{n_\ell(kR)} \frac{1}{A_\ell}. \tag{2.17}$$

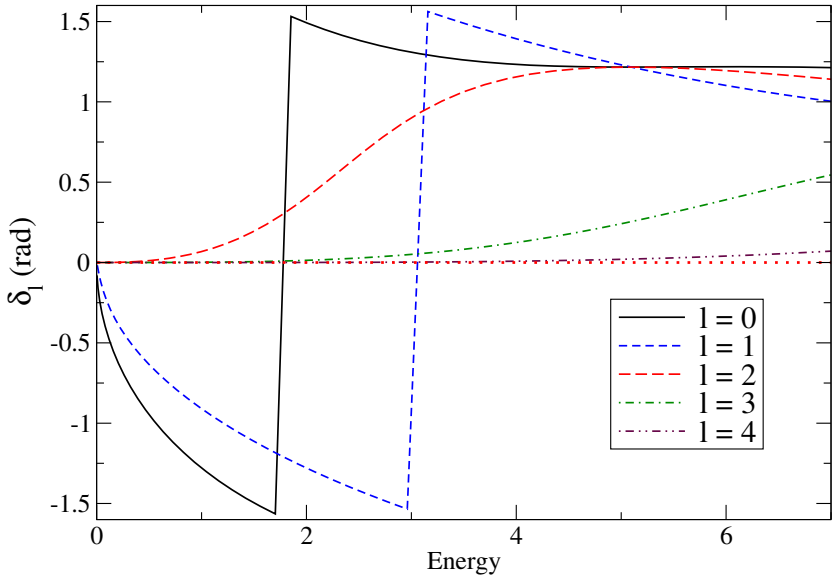

Figure 2.4: Phase shift δ_ℓ (in radians) for a square well with $m = \hbar = R = 1$, well depth V_0=5, versus energy $= \hbar^2 k^2/2m$, for different angular momentum ℓ. The dotted red line at $\delta = 0$ is to guide the eye.

and then

$$K\left(-j_{\ell+1}(KR) + \frac{\ell+1}{KR} j_\ell(KR)\right) = k\left[A_\ell\left(-j_{\ell+1}(kR) + \frac{\ell+1}{kR} j_\ell(kR)\right)\right.$$
$$\left. - \frac{(A_\ell j_\ell(kR) - j_\ell(KR))}{n_\ell(kR)}\left(-n_{\ell+1}(kR) + \frac{\ell+1}{kR} n_\ell(kR)\right)\right]$$

Now, with some algebra, we can solve for A_ℓ and finally we get the phase shift,

$$\tan\delta_\ell = \frac{kj_\ell(KR)j_{\ell+1}(kR) - Kj_\ell(kR)j_{\ell+1}(KR)}{kj_\ell(KR)n_{\ell+1}(kR) - Kn_\ell(kR)j_{\ell+1}(KR)} \tag{2.18}$$

This can be tested by checking the case $\ell = 0$, with

$$j_0(x) = \frac{\sin x}{x}, \quad j_1(x) = \frac{\sin x - x\cos x}{x^2}$$
$$n_0(x) = -\frac{\cos x}{x}, \quad n_1(x) = -\frac{\cos x + x\sin x}{x^2}$$

and indeed it reduces to the correct answer,

$$\tan\delta_0 = \frac{k\tan KR - K\tan kR}{K + k\tan kR\tan KR}. \tag{2.19}$$

To see how the phase shifts vary with ℓ, see Fig. 2.4. Notice as ℓ increases, the phase shifts decrease. This makes sense, because scattering at higher angular momentum is of necessity more peripheral, and hence, the effect of the potential is lessened. The phase shifts for $\ell = 0, 1$ start off negative because they both have one bound state, while $\ell = 2, 3, \ldots$ do not have bound states.

Exercise 2.3. Confirm for yourself Eqn. (2.18) and that for $\ell = 0$ we regain (2.19).

2.3 Phase shifts and cross-sections: formal derivation

Now that we have some examples of phase shifts, we ask: how do phase shifts affect the cross-section? Here's the short answer: We've decomposed the wave-function into pieces with good angular momentum ℓ, the so-called *partial waves*. In the absence of a scattering potential, the sum all the partial waves for the projectile is a plane wave. In the presence of a scattering potential, each partial wave undergoes a shift in phase, which in turn causes an interference pattern which causes the probability to depend upon the angle–the cross-section. The rest of this section works out these relations in depth. This is the starting point for many introductory texts, so it's possible you have seen this before.

First, let's start with the incoming plane wave, and assume that the momentum $\vec{p}$ and the wave vector $\vec{k}$ are both in the z-direction. Then the plane wave is

$$\exp(i\vec{k} \cdot \vec{r}) = \exp(ikz) = \exp(ikr\cos\theta), \tag{2.20}$$

where in the last step I've moved into spherical coordinates. We can expand any function in spherical coordinates into spherical harmonics, that is,

$$\exp(ikr\cos\theta) = \sum_{\ell,m} g_{\ell,m}(r) Y_{\ell,m}(\theta, \phi); \tag{2.21}$$

except we know there is no ϕ-dependence, so we only need $m = 0$, and $Y_{\ell,m}(\theta, \phi) = P_\ell(\cos\theta)$ the Legendre polynomial (up to some constant), and so

$$\exp(ikr\cos\theta) = \sum_{\ell} g_\ell(r) P_\ell(\theta). \tag{2.22}$$

As discussed in the last section, however, we also know that the solutions to the free Schrödinger equation for angular momentum ℓ are spherical Bessel and spherical Neumann functions, and that only the former is regular at the origin. Hence we must have

$$\exp(ikr\cos\theta) = \sum_{\ell} c_\ell j_\ell(kr) P_\ell(\theta). \tag{2.23}$$

With some more analysis, one can finally arrive at

$$\exp(ikr\cos\theta) = \sum_\ell i^\ell (2\ell+1) j_\ell(kr) P_\ell(\theta). \tag{2.24}$$

This expansion is important for us, not only because it will lead us to phase shifts, but also because we will come back and use this expansion for the asymptotic normalization for scattering states.

Next, we expand the scattering amplitude $f(\theta)$ in a similar way:

$$f(\theta) = \sum_\ell (2\ell+1) a_\ell(k) P_\ell(\cos\theta) \tag{2.25}$$

where $a_\ell(k)$ is a partial scattering amplitude. Because the differential cross section is

$$\frac{d\sigma}{d\Omega} = |f(\theta)|^2, \tag{2.26}$$

if we expand in partial amplitudes and integrate over θ, or rather $x = \cos\theta$, using

$$\int_{-1}^{1} dx P_\ell(x) P_{\ell'}(x) = \frac{2}{2\ell+1}\delta_{\ell\ell'}.$$

we get the total cross-section,

$$\sigma = \int \frac{d\sigma}{d\Omega} d\Omega = 4\pi \sum_\ell (2\ell+1)|a_\ell(k)|^2 \tag{2.27}$$

With these expansions in mind, consider the full scattering wave function, complete with both incoming and outgoing parts, at large r:

$$\psi_{\text{scatt}} \underset{r\to\infty}{\to} e^{ikz} + f(\theta)\frac{e^{ikr}}{r} = \sum_\ell \left[i^\ell j_\ell(kr) + a_\ell(k)\right](2\ell+1)P_\ell(\theta). \tag{2.28}$$

But at large r, we know

$$j_\ell(kr) \underset{r\to\infty}{\to} (kr)^{-1}\sin\left(kr - \frac{\ell\pi}{2}\right) = \frac{1}{2ikr}\left[e^{ikr}e^{-i\frac{\ell\pi}{2}} - e^{-ikr}e^{+i\frac{\ell\pi}{2}}\right], \tag{2.29}$$

which is another way of saying a plane wave is a combination of incoming and outgoing *spherical* waves. Using this expansion, we get

$$\psi_{\text{scatt}} \underset{r\to\infty}{\to} \frac{1}{2ik}\sum_\ell \left[(1+2ik\,a_\ell(k))\,\frac{e^{ikr}}{r} - \frac{e^{-i(kr-\ell\pi)}}{r}\right](2\ell+1)P_\ell(\theta). \tag{2.30}$$

There is another way to look at the asymptotic behavior, however, in terms of phase shifts: we know that $u_\ell(k,r) = \sin\left(kr - \frac{\ell\pi}{2} + \delta_\ell(k)\right)$, and putting in some

amplitude, we have

$$\psi_{\text{scatt}} \underset{r\to\infty}{\to} \frac{1}{r}\sum_\ell c_\ell \sin\left(kr - \frac{\ell\pi}{2} + \delta_\ell(k)\right) P_\ell(\theta) \tag{2.31}$$

$$= \frac{1}{2ir}\sum_\ell c_\ell \left[\exp\left(i\left(kr - \frac{\ell\pi}{2} + \delta_\ell\right)\right) - \exp\left(-i\left(kr - \frac{\ell\pi}{2} + \delta_\ell\right)\right)\right] P_\ell(\cos\theta). \tag{2.32}$$

Matching the terms in (2.28) and (2.32) in front of the incoming spherical wave $\exp(-ikr)/r$, we get

$$\frac{c_\ell}{2i} = \frac{2\ell+1}{2ik}\exp\left(i\left(\delta_\ell + \frac{\ell\pi}{2}\right)\right). \tag{2.33}$$

Finally, matching the terms in front of the outgoing spherical wave $\exp(+ikr)$ and using (2.33), we arrive at

$$1 + 2ik\, a_\ell(k) = e^{2i\delta_\ell(k)}. \tag{2.34}$$

Often we call $e^{2i\delta_\ell}$ and its generalizations the *scattering* or S-matrix. While it seems abstract, it has many poweful properties we can exploit. Solving further for the partial amplitudes,

$$a_\ell(k) = \left(\frac{e^{2i\delta_\ell} - 1}{2ik}\right) = \frac{e^{i\delta_\ell}\sin\delta_\ell}{k}. \tag{2.35}$$

Now we can see what the scattering amplitude $f(\theta)$ is: then interference between in the incoming plane wave and the phase-shifted scattered outgoing spherical wave. If the phase shifts are zero, there is no scattering amplitude. We can rewrite the total cross section as

$$\sigma = \sum_\ell 4\pi(2\ell+1)\frac{\sin^2\delta_\ell(k)}{k^2}. \tag{2.36}$$

Notice that for any ℓ, the maximum contribution is when $\delta_\ell = \frac{\pi}{2} \pm n\pi$. This is called the *unitary limit* and will be important when we talk about *resonances* and related topics.

We can rewrite the partial scattering amplitude in different ways that will prove useful. For example,

$$a_\ell = \frac{e^{i\delta_\ell}\sin\delta_\ell(k)}{k} = \frac{\sin\delta_\ell(k)}{ke^{-i\delta_\ell}} = \frac{\sin\delta_\ell(k)}{k(\cos\delta_\ell - i\sin\delta_\ell)} = \frac{1}{k\cot\delta_\ell(k) - ik}. \tag{2.37}$$

Then, for example, we can write

$$\sigma = \sum_\ell \frac{4\pi(2\ell+1)}{k^2 + k^2\cot^2\delta_\ell(k)}. \tag{2.38}$$

In the next figure, I plot the $\ell = 0$ contribution to the square well for some set of parameters. Notice the big bump; that is a *resonance*, which we will explore more in the next Chapter. (Well, no, the square well does not have any resonances in the s-wave.)

2.4 Scattering lengths and the effective range expansion

For $\ell = 0$,

$$k \cot \delta_0 = -\frac{1}{a} + \frac{1}{2} r_0 k^2 + \ldots, ... \tag{2.39}$$

where a is the *scattering length* and r_0 is the *effective range*. This is particularly useful, because in the limit as $k \to 0$, only the s-wave channel contributes and the total cross section at $k = 0$, also called *at threshhold*, is

$$\lim_{k \to 0} \sigma = 4\pi a^2. \tag{2.40}$$

Example: the hard sphere. The $\ell = 0$ phase shift for a hard sphere of radius R is $\delta_0 = kR$, hence $a = -R$. This means the total cross section at threshhold is $4\pi R^2$, which is the total surface area of the hard core. At first this seems strange; naively you might expect the cross-section to be πR^2. But as $k \to 0$, the wavelength becomes longer and longer and the wave function of the scattering particle "wraps around" the entire sphere.

Exercise 2.4. Show for the hard core the effective range $r_0 = -R/3$.

Example: the finite square well. Starting from (2.14), we can write

$$\tan \delta_0 = \tan \left[-kR + \tan^{-1} \left(\frac{k}{K} \tan KR \right) \right].$$

Now we use a trig identity, $\tan(A - B) = (\tan A - \tan B)/(1 + \tan A \tan B)$ to get

$$\cot \delta_0 = \frac{K + k \tan kR \tan KR}{k \tan KR - K \tan kR}$$

Using $K = \sqrt{k^2 + K_0^2}$ with $K_0 = \sqrt{2mV_0}/\hbar$, we finally have

$$k \cot \delta_0 = \frac{\sqrt{k^2 + K_0^2} + k \tan kR \tan \sqrt{k^2 + K_0^2} R}{\tan \sqrt{k^2 + K_0^2} R - \sqrt{1 + K_0^2/k^2} \tan kR} \tag{2.41}$$

Expanding up to second order in k (you may use Mathematica or MatLab or any other symbolic manipulation program), we get

$$k \cot \delta_0 = \frac{K_0}{\tan K_0 R - K_0 R}$$
$$+ \frac{1}{2} k^2 K_0^{-1} \frac{\tan K_0 R (1 - 2(K_0 R)^2) - K_0 R - 2 K_0 R \tan^2 K_0 R + \frac{2}{3} (K_0 R)^3}{(\tan K_0 R - K_0 R)^2} \tag{2.42}$$

so that the scattering length is

$$a = R - \frac{\tan K_0 R}{K_0} \tag{2.43}$$

and the effective range is

$$r_0 = K_0^{-1} \frac{(1 - 2(K_0R)^2) \tan K_0R - K_0R - 2K_0R \tan^2 K_0R + \frac{2}{3}(K_0R)^3}{(\tan K_0R - K_0R)^2} \tag{2.44}$$

If we define the dimensionless parameter $X = K_0R$ then

$$a = R\left(1 - \frac{\tan X}{X}\right) \tag{2.45}$$

and

$$r_0 = K_0^{-1} \frac{(1 - 2X^2) \tan X - X - 2X \tan^2 X + \frac{2}{3}X^3}{(X - \tan X)^2} \tag{2.46}$$

While the scattering length can be positive or negative, if you take a Taylor series expansion for r_0, you will find to very high order all the terms are (???) positive:

$$r_0 = K_0^{-1}\left(9 + 2X^2 + \frac{68}{105}X^4 \ldots\right) \tag{2.47}$$

You may notice that if $K_0R = n\pi/2$ for any odd integer n, the scattering length becomes infinite. This is known as the *unitary limit*, in part because it saturates the cross-section.

For shallow wells, X is small, and $1 - \tan(x)/x \approx x^2/3$, and

$$a \approx \frac{2}{3}\frac{mV_0R^3}{\hbar^2}.$$

that is, the scattering length increases linearly with the depth and with the volume of the well.

Exercise 2.5. Derive the scattering length for the square well, (2.43). Plot for various values of R and V_0.

Exercise 2.6. Derive the effective for the square well, (2.44). *Hard.*

Can one generalize for higher angular momenta ℓ? Yes, although the interpretations are less natural. For example, one can show for the hard sphere,

$$\lim_{k\to 0} \tan\delta_\ell(k) = -\left(\frac{2^\ell \ell!}{(2\ell)!}\right)^2 (kR)^{2\ell+1} \tag{2.48}$$

Thus one could expand around $k^{2\ell+1}\cot\delta_\ell$ but the $k \to 0$ term would have units of $(\text{length})^{2\ell+1}$, which makes it less intuitive.

Exercise 2.7. For the square well, compute

$$\lim_{k\to 0} -\frac{\tan\delta_\ell(k)}{k^{2\ell+1}}$$

which is the equivalent of the scattering length for all ℓ. **Hard.**

2.5 Another analytic example: the δ-shell potential

There are relatively few scattering potentials which are both analytically and numerically tractable. For example, the hard core is easy analytically, but for technical reasons is not tractable when we try harmonic oscillator space methods below.

In addition to the square well, which has been our focus so far, I want to add another example, the δ-shell potential, which has a δ-function at a radius R from the origin, that is,

$$V(r) = \lambda\delta(r-R).$$

Before we start calculating with this, let's do some dimensional analysis. Because the δ-function has units of inverse length, λ has units of energy $\times$ length. Furthermore, it will become convenient to write not in terms of energy but in in terms of some inverse length k_0, with energy $\hbar^2k_0^2/2m$. Putting together, we choose

$$V(r) = \frac{\hbar^2 k_0}{2m}\delta(r-R), \tag{2.49}$$

where k_0 has dimensions of inverse length, but can be positive or negative.

To solve for $\ell = 0$, we break up $u(r)$ into two regions:

$$\begin{aligned} u(r) &= \sin kr, & 0 \le r \le R,\\ u(r) &= A\sin(kr+\delta), & R \le r. \end{aligned}$$

We match the wave functions at $r = R$, given $A = \sin(kR)/(\sin(kR+\delta))$. We do not, however, match derivatives, because the potential is infinite at $r = R$ and this causes a discontinuity in the first derivative. Following the procedure for the bound state of a δ-potential in one dimension, a standard topic in most texts, we instead integrate over the discontinuity. Solving, we arrive at (this should be checked!)

$$\tan\delta_0 = -\frac{k_0\sin^2(kR)}{k + k_0\sin(kR)\cos(kR)} \tag{2.50}$$

Expanding $k\cot\delta$ we get the scattering length

$$a = -R\frac{k_0R}{k_0R+1}, \tag{2.51}$$

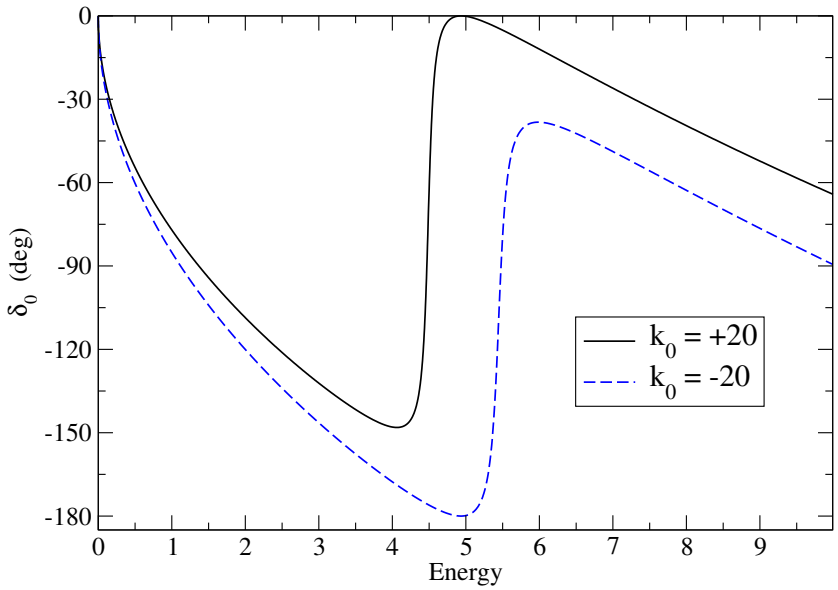

Figure 2.5: s-wave phase shifts (in degrees) for the δ-shell potential at a distance $R = 1$, versus energy with $\hbar = m = 1$.

and the effective range

$$r_{\text{eff}} = \frac{2}{3}\frac{k_0 R - 1}{k_0} \tag{2.52}$$

(Both of these should be checked!)

Fig. 2.5 shows representative phase shifts, in degrees, for $m = \hbar = 1$ and the distance $R = 1$ for the parameter $k_0 = \pm 20$. (If you happen to wonder if there is a rule for phase shifts to be positive or negative, there is none. The most physical convention is that all phase shifts vanish as $k \to 0$. Also, phase shifts may be given in degrees or radians; I am switching between them both so you get used to asking the question!

Exercise 2.8. For the δ-shell potential with $k_0 < 0$ (attractive), investigate the ground state energy. Show that the condition for a bound ground state is

$$\kappa = |k_0| \left(1 - \exp(-2\kappa R)\right)/2, \tag{2.53}$$

where $\kappa = \sqrt{2m|E_b|}/\hbar$, with $E_b < 0$ is the bound ground state energy. For κR large, this leads to

$$E_b \approx -\frac{\hbar^2 k_0^2}{8m}.$$

Confirm these results.

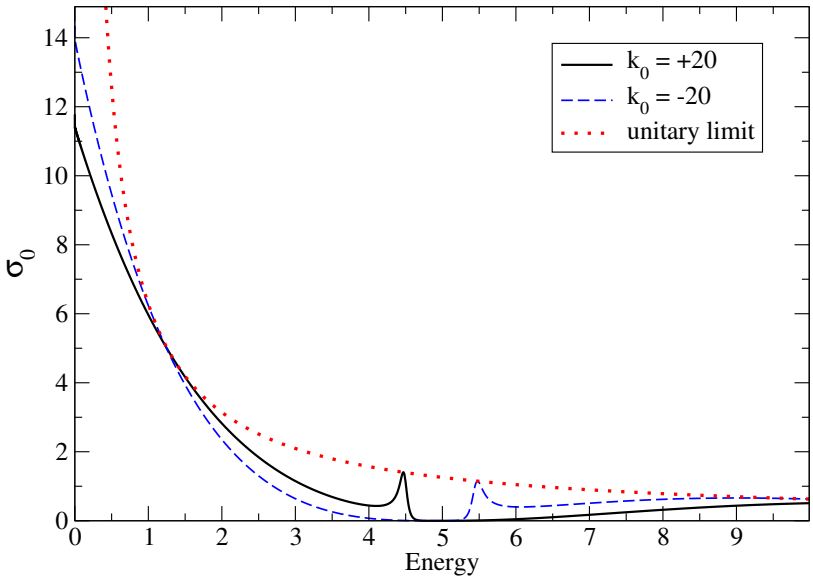

Figure 2.6: s-wave cross-section for the δ-shell potential at a distance $R = 1$, versus energy with $\hbar = m = 1$, with the unitary limit (red dotted line) shown to guide the eye.

2.6 Resonances: a first look

In Fig. 2.6 I plot the cross-sections for the the δ-shell potential for a couple of representative strengths. You'll note a fairly sharp bump around 4.5 for $k_0 = +20$ and around 5.5 for $k_0 = -20$. These are examples of *resonances*, an important phenomenon in scatteringand reactions; in many physical situations we find resonances, either with broad or narrow peaks. Physically, resonances are a significant rise, then fall, in cross section, often reaching the unitary limit. Mathematically, resonances are when the phase shift passes through $\pi/2$ swiftly, as we see happening in Fig. 2.6.

We can see in more detail what is happening in Fig. 2.7, where I plot $k \cot \delta_0$. In the previous examples I've given, $k \cot \delta_0$ looked like a smooth polynomial, nearly linear. But of course, as $\delta_0 \to \pm\pi/2$, $\cot \delta_0 \to \pm\infty$. In the next chapter we will investigate this via the poles of the S-matrix in the complex momentum plane, and be able to derive a rigorous mathematical representation for this quite common phenomenon.

Unfortunately resonances are difficult to create in analytic cases. The square well does not have any s-wave resonances at finite energy. They occur in more complex potentials and in many-body scattering and reactions. We will return to resonances later.

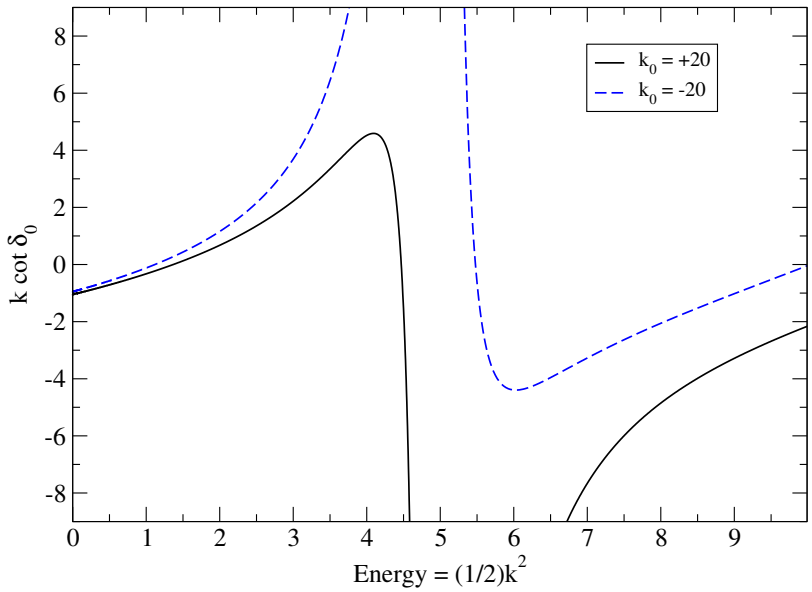

Figure 2.7: $k \cot \delta_0$ for the δ-shell potential at a distance $R = 1$, versus energy with $\hbar = m = 1$.

2.7 Project 2: A first look at data

Project 2. In each chapter I will introduce one or more detailed projects that go beyond the exercises, although often the code you use for the exercises will be useful for the projects and *vice versa*.

Even though this first part of the book is mostly analytic, it is never too early to start getting your hand dirty on data. We will focus on nuclear data. Table 2.1 gives experimental neutron-proton phase shifts. We won't worry about error bars yet.

It is important here to take note of *spectroscopic notation*. I assume the reader is generally familar with the rules for adding angular momentum in

Table 2.1: Proton-neutron phase shifts in degrees. Energies are in MeV.

$E_{\rm lab}$	$^3S_1$	$^1P_1$	$^1S_0$	$^3P_0$
1	147.75	-0.19	62.02	0.18
5	118.18	- 1.51	63.50	1.64
10	102.62	-3.11	59.78	3.71
25	80.68	-6.48	50.61	8.32
50	62.89	-9.85	40.09	10.99
100	43.51	-14.20	26.02	8.69
150	31.19	-17.68	15.98	3.78

quantum mechanics, and the difference between intrinsic spin s or S, $= 1/2$ for electrons, protons, and neutrons, orbital angular momentum ℓ or L, and total angular momentum j or $J = |\ell \pm 1/2|$. (If you are not, *put this book aside now* and read about it in your favorite introductory quantum mechanics text.)

For two identical spin-1/2 fermions, the total spin is $S = 0$ or 1. (We typically though not always use lower-case letters for single particles and capital letters for two or more particles.) The total angular momentum is denoted L and by tradition one uses S to denotes $L = 0$, P to denotes $L = 1$, D to denote $L = 2$, F for $L = 3$, G for $L = 4$, and afterwards alphabetically. The relative angular momentum is written as ${}^{2S+1}(L)_J$, so that ${}^3S_1$ means $L = 0$, $S = 1$ and $J = 1$, and is pronounced "triplet-S," while ${}^1D_2$ means $L = 2$, $S = 0$ and $J = 2$.

In nuclear physics there is an additional quantum number, isospin, which acts like spin: protons and neutrons each have isospin 1/2, while a pair of nucleons have either isospin $T = 0$ or 1. Isospin is not exactly conserved, but it is a "good enough" quantum number to help guide our thinking.

Due to antisymmetry, we must have $(-1)^{L+S+T} = -1$. Thus, in Table 2.1, ${}^3S_1$ and ${}^1P_1$ are $T = 0$ and ${}^1S_0$ and ${}^3P_0$ are $T = 1$.

For the ${}^3S_1$ and ${}^1S_0$ channels, plot $k \cot \delta$, and extract the scattering lengths and effective ranges. (I talk about polynomial fits later on, but for now most graphing software allow for some sort of linear regression.) For ${}^1P_1$ and ${}^3P_0$ plot $k^3 \cot \delta$ and extract the y-intercepts and slopes.

Chapter 3

Introducing the S-matrix

One of the fundamental concepts in scattering theory is the scattering or S-matrix. The basic idea is simple: one aims a projectile at a target or interaction region, which is then scattered. We conceptualize "inbound" and "outbound" wave functions, and the S-matrix connects the two:

$$\Psi^{\text{out}} = \hat{S}\Psi^{\text{in}}.$$

To do this we have to set up the math to explain exactly what we mean by "inbound" and "outbound." Because there is a lot of formal development, you can skip this chapter and return to it as needed.

What you should know: the S-matrix should be unitary, which makes sense as one should conserve particles. Sometimes we encounter apparent exceptions, in the case of absorbtion or reactions. In those cases, however, we have simple truncated our Hilbert space which leads to the apparent non-unitarity. More on this later.

In the case of elastic scattering, momentum is conserved, hence the S-matrix is diagonal in momentum space, and as it is a unitary matrix, the elements of the momentum-space S-matrix are just complex numbers of modulus one, which we write as

$$S(k) = e^{2i\delta(k)} \tag{3.1}$$

where $\delta(k)$ will turn out to be, of course, the phase shift.

3.1 Green's functions and the Lippmann-Schwinger equation

To find the quantum wave function we want to solve the Schrödinger equation,

$$\hat{H}|\Psi\rangle = E|\Psi\rangle. \tag{3.2}$$

In many cases, however, it is not possible to solve the Schrödinger equation directly and we must turn to approximate methods. A powerful way to set up ap-

proximate solutions is through *Green's functions* and the *Lippmann-Schwinger equation*.

Green's functions are a standard way to solve differential equations, and we only brief survey them here; as always, see your favorite math methods text for more details. Let $\hat{\mathcal{L}}$ be some linear (differential) operator. We call

$$\hat{\mathcal{L}}|\Phi_0\rangle = 0 \tag{3.3}$$

a *homogeneous* equation and

$$\hat{\mathcal{L}}|\Phi\rangle = |f\rangle \tag{3.4}$$

an *inhomogeneous* equation, with $|f\rangle$ the *source* term. To solve the latter, we introduce the *Green's function* $\hat{\mathcal{G}}$ which is formally the inverse of the operator,

$$\hat{\mathcal{L}}\hat{\mathcal{G}} = \mathbf{1}. \tag{3.5}$$

Then the general solution is

$$|\Phi\rangle = |\Phi_0\rangle + \hat{\mathcal{G}}|f\rangle, \tag{3.6}$$

as we can arbitrarily add a homogeneous solution.

In quantum mechanics, we use Green's functions to tackle problems we cannot solve fully. Suppose we cannot solve (3.2), but for another Hamiltonian, $\hat{H}_0$, we do know the solutions:

$$\hat{H}_0|\Psi_0\rangle = E|\Psi_0\rangle. \tag{3.7}$$

Typically $\hat{H}_0$ is the Hamiltonian for the free particle, or for the harmonic oscillator. If we write $\hat{H} = \hat{H}_0 + \hat{V}$, then we rewrite

$$\hat{H}|\Psi\rangle = \left(\hat{H}_0 + \hat{V}\right)|\Psi\rangle = E|\Psi\rangle$$

as

$$\left(\hat{H}_0 - E\right)|\Psi\rangle = \hat{V}|\Psi\rangle. \tag{3.8}$$

In this case the right hand side, $\hat{V}|\Psi\rangle$, plays the role of the source term. We now introduce the Green's function

$$\hat{G}_0(E) = \left(\hat{H}_0 - E\right)^{-1} \tag{3.9}$$

sometimes called the "free" Green's function when $\hat{H}_0$ is the kinetic energy (free-particle Hamiltonian), and now can write

$$|\Psi\rangle = |\Psi_0\rangle + \hat{G}_0(E)|\Psi\rangle = |\Psi_0\rangle + \frac{1}{\hat{H}_0 - E}|\Psi\rangle, \tag{3.10}$$

where, again, $|\Psi_0\rangle$ is an "homogeneous" solution, which here is the solution (3.7). This is the Lippmann-Schwinger equation. As we'll see, it is the starting point for approximate solutions, including perturbation theory, Feynmann

diagrams for quantum field theory (which is itself perturbation theory), and, relevant to us, scattering theory.

Eqn. (3.10) is most often solved iteratively, starting with the homogeneous or "free" solution, that is, as a sequence of approximations $|\Psi^{(I)}\rangle$ which are fed into the next iteration:

$$|\Psi^{(0)}\rangle = |\Psi_0\rangle, \tag{3.11}$$

$$|\Psi^{(1)}\rangle = |\Psi_0\rangle + \hat{G}_0(E)\hat{V}|\Psi^{(0)}\rangle = |\Psi_0\rangle + \hat{G}_0(E)\hat{V}|\Psi_0\rangle, \tag{3.12}$$

$$|\Psi^{(2)}\rangle = |\Psi_0\rangle + \hat{G}_0(E)\hat{V}|\Psi_0\rangle + \hat{G}_0(E)\hat{V}\hat{G}_0(E)\hat{V}|\Psi_0\rangle, \tag{3.13}$$

$$\begin{aligned}|\Psi^{(3)}\rangle = |\Psi_0\rangle + \hat{G}_0(E)\hat{V}|\Psi_0\rangle + \hat{G}_0(E)\hat{V}\hat{G}_0(E)\hat{V}|\Psi_0\rangle \\ +\hat{G}_0(E)\hat{V}\hat{G}_0(E)\hat{V}\hat{G}_0(E)\hat{V}|\Psi_0\rangle,\end{aligned} \tag{3.14}$$

$$\dots$$

Note that this assumes that both $|\Psi_0\rangle$ and $|\Psi\rangle$ have the same energy, E; thus the Lippmann-Schwinger equation is usually applied to continuum solutions, and furthermore is not well suited for methodologies with discretized continua.

3.2 Derivation of Green's functions

First, let's derive a Green's function in one dimension. Consider the one-dimensional, time-independent Schrödinger equation,

$$-\frac{\hbar^2}{2M}\frac{d^2}{dx^2}\psi(x) + V(x)\psi(x) = E\psi(x) = \frac{\hbar^2 k_0^2}{2M}\psi(x),$$

which I rewrite as

$$\left(\frac{d^2}{dx^2} + k_0^2\right)\psi(x) = \frac{2M}{\hbar^2}V(x)\psi(x), \tag{3.15}$$

an obvious candidate for a Green's function.

There are at least two different ways to get the Green's function. The first is to use Sturm-Liouville theory, which will be written up at a later date. Instead I turn to spectral decomposition, which means expanding in eigenstates of $\mathcal{L}$. Here that means a Fourier expansion.

Introducing the Green's function $G(x, x') = G(x - x')$, consider its Fourier transform,

$$\tilde{G}(k) = \int_{-\infty}^{\infty} e^{-ikx}G(x)\,dx, \tag{3.16}$$

and the inverse,

$$G(x) = \frac{1}{2\pi}\int_{-\infty}^{\infty} e^{+ikx}\tilde{G}(k)\,dk. \tag{3.17}$$

The Fourier transform of the Dirac δ-function, $\delta(x)$, is 1, and the Fourier transform of

$$\frac{d^2}{dx^2} + k_0^2$$

is $-k^2 + k_0^2$. Hence in Fourier space, $\left(-k^2 + k_0^2\right) \tilde{G}(k) = 1$, or

$$\tilde{G}(k) = \frac{1}{k_0^2 - k^2}, \tag{3.18}$$

and, formally,

$$G(x) = \frac{1}{2\pi} \int_{-\infty}^{\infty} e^{ikx} \frac{1}{k_0^2 - k^2} dk. \tag{3.19}$$

I say "formally" because this integral has some subtlety in its evaluation. Most importantly, it blows up at $k = \pm k_0$. How do we handle that? We invoke integrals in the complex k-plane and Cauchy's theorem.

First note that

$$\frac{1}{k_0^2 - k^2} = \frac{1}{2k_0} \left(\frac{1}{k + k_0} - \frac{1}{k - k_0} \right) \tag{3.20}$$

This explicitly points out the simple poles at $k = \pm k_0$.

The solution to the exploding integral is to shift the integral slightly into the complex k-plane and do a contour integral. (Refer to the appendix and to your favorite math methods text for more details.) That is, we let $k_0 \to k_0 \pm i\epsilon$ as $\epsilon \to 0^+$, which means ϵ goes to zero, but only from the positive side. The choice of adding or subtracting $i\epsilon$ will implicitly lead to a boundary condition.

As a reminder, in the complex z-plane, at or near a simple pole z_0 a function $f(z)$

$$f(z) \to \frac{\mathrm{Res} f(z_0)}{z - z_0} \tag{3.21}$$

where $\mathrm{Res} f(z_0)$ is the *residue* of the function at the pole, and is just

$$\mathrm{Res} f(z_0) = \lim_{z \to z_0} (z - z_0) f(z). \tag{3.22}$$

We say z_0 is a simple pole if the residue at z_0 is nonzero.

The Cauchy residue theorem is

$$\oint f(z)\, dz = 2\pi i \times \sum_{k \in \circ} \mathrm{Res}(f(z_k)) \tag{3.23}$$

where $\oint$ means a closed, counter-clockwise (the sense is important), contour integral, and $k \in \circ$ means all poles enclosed by the contour.

The integral (3.19) is along the real k axis. We choose the contour integral to either be closed in the upper half plane (see figure, to be added), or in the lower half plane. We choose either uppper or lower half plane so that the arc for large $\pm \mathrm{Im}\, k$ vanishes. In this case, the function to be integrated is

$$f(k) = \frac{e^{ikx}}{k_0^2 - k^2},$$

with the numerator dominated away from the poles. As k is complex, $\exp(ikx) = \exp(i(\mathrm{Re}\, k)\, x) \times \exp(-(\mathrm{Im}\, k)\, x)$. We want $(\mathrm{Im}\, k)\, x > 0$ to suppress contributions away from the real k-axis. Hence if $x > 0$, choose $\mathrm{Im}\, k > 0$, which is the upper half plane, and if $x < 0$, choose $\mathrm{Im}\, k < 0$, the lower half plane.

As I said above, the choice of sign on $i\epsilon$ implicitly leads to boundary conditions. I will now show this in detail. First, consider shifting $k_0 \to k_0 + i\epsilon$, so there are poles at $\pm(k_0 + i\epsilon$. [Insert picture here]

For $x > 0$, which implies a contour in the upper half plane, we take the reside at $+k_0$; the residue at $-k_0$ is outside the contour. In addition, in order to draw the contour from $-\infty$ to $+\infty$ along the real k axis, and then cross back along the upper half plane, the contour is clock-wise. As Cauchy's residue theorem is for counter-clockwise contours, this means we pick up an addition $-$ sign in the integration. For $x < 0$, the residue is at $-k_0$, the contour is in the lower half-plane. Thus, in the integral representation for the Green's function,

$$G(x) = \frac{1}{2\pi}\frac{1}{2k_0}\int e^{ikx}\left(\frac{1}{k+k_0} - \frac{1}{k-k_0}\right)dk, \tag{3.24}$$

the first term in the parentheses contributes only for $x < 0$, and the second terms only for $x > 0$.

Evaluating the integral in two regimes:

$x > 0$:

$$G(x) = \frac{1}{2\pi}\frac{1}{2k_0}2\pi i(-1)(-e^{i(+k_0)x}), \tag{3.25}$$

where $-e^{ik_0x}$ is the residue at $k = +k_0$, and the (-1) is for the clockwise contour, and

$x < 0$:

$$G(x) = \frac{1}{2\pi}\frac{1}{2k_0}2\pi i(+e^{i(-k_0)x}), \tag{3.26}$$

with the residue evaluates at $k = -k_0$.

Putting this all together,

$$G(x) = \frac{i}{2k_0}e^{ik_0|x|}. \tag{3.27}$$

I promised an interpretation in terms of boundary conditions. When we apply the Green's function, we have

$$\psi(x) = \int G(x - x')\psi_0(x')\, dx'. \tag{3.28}$$

Assume $\psi_0(x')$ is localized, and consider $x \gg x'$, that is, we look far to the *right* of our source. Then $G(x - x') = (i/2k_0)e^{ik_0x}e^{-ik_0x'}$ and

$$\psi(x) \approx e^{ik_0x} \times \left[\frac{i}{2k_0}\int e^{-ik_0x'}\psi_0(x')\, dx'\right], \tag{3.29}$$

that is, we get a *right-going* wave out. If we switch the assumption so that $x \gg x'$, so that we look far to the left of our source we get

$$\psi(x) \approx e^{-ik_0 x} \times \left[\frac{i}{2k_0} \int e^{ik_0 x'} \psi_0(x')\, dx' \right], \tag{3.30}$$

a left-going wave. Hence our interpretation is that this Green's function generates waves *outgoing* from the source.

If, instead, we choose $k_0 - i\epsilon$, we would end up with

$$G(x) = -\frac{i}{2k_0} \exp\left(-ik_0|x|\right), \tag{3.31}$$

which corresponds to incoming waves, that is, towards the source.

Let's apply this to an example: transmission through a one-dimensional square well.

3.3 Free-particle Green's function in three dimensions

Fresh off the success of finding the free-particle Green's function in one dimension, let's turn to three dimensions. The equation for the Green's function is

$$\left(\nabla^2 + k_0^2\right) G(\vec{r} - \vec{r'}) = \delta^{(3)}(\vec{r} - \vec{r'}). \tag{3.32}$$

(Some developments have $-\delta^{(3)}(\vec{r} - \vec{r'})$, to get rid of a $-$ sign later on.) In Fourier space this is

$$(-k^2 + k_0^2)\tilde{G}(\vec{k}) = 1. \tag{3.33}$$

Therefore, as in one dimension,

$$G(\vec{r} - \vec{r'}) = G(\vec{x}) = \frac{1}{(2\pi)^3} \int d^3k\, \frac{\exp(i\vec{k} \cdot \vec{x})}{-k^2 + k_0^2}. \tag{3.34}$$

We can choose $\vec{k}$ to point in any convenient direction, so let's choose the z direction. Then Then $\vec{k} \cdot \vec{x} = kx\cos\theta = kxu$, and integrating over θ, or more easily u, as well as trivially over ϕ, to get

$$\frac{1}{2\pi^2} \frac{1}{x} \int_0^\infty dk\, \frac{k \sin kx}{-k^2 + k_0^2} \tag{3.35}$$

Note the integrand is even in k, so we can rewrite this as

$$\frac{1}{4\pi^2} \frac{1}{x} \int_{-\infty}^\infty dk\, \frac{k \sin kx}{-k^2 + k_0^2} = \frac{1}{4ix\pi^2} \int_{-\infty}^\infty dk\, \frac{k e^{ikx}}{-k^2 + k_0^2} \tag{3.36}$$

as only the even part of the integrand will survive.

The rest of the analysis is similar to that in one dimension. Note that here, $x = |\vec{r} - \vec{r}'| \geq 0$ always. If we choose poles at $\pm(k_0 + i\epsilon)$, then for $\exp(ikx)$ to vanish far away from the real k axis, we must have $\mathrm{Im}\, k > 0$, and hence close the (counter-clockwise) contour in the upper half plane. Thus we evaluate the pole at $k = +k_0$ and get

$$G(x) = \frac{1}{4i\pi^2 x} 2\pi i(-1) \frac{1}{2k_0}(+k_0) e^{i(+k_0)x} = -\frac{1}{4\pi x} e^{ik_0 x}, \tag{3.37}$$

or

$$G(\vec{r}, \vec{r}') == -\frac{1}{4\pi|\vec{r} - \vec{r}'|} \exp\left(ik_0|\vec{r} - \vec{r}'|\right), \tag{3.38}$$

which is a wave going out and away from the origin.

3.4 Mathematical interlude: Sturm-Liouville problems

Any second-order linear differential equation (this is known as a Sturm-Liouville problem) has two solutions, and one choose between them through a boundary condition.

3.5 Radial Green's functions

Using what we learned in the last section, we can now derive Green's functions for the radial part of a wave function.

3.6 Jost functions

Jost functions are another way to arrive at the S-matrix and, in particular, to consider complex momenta. While this may seem like a wild idea, it turns out to be very useful.

To begin with, recall that for large r, the solution to the radial Schrödinger equation with momentum $p = \hbar k$

$$u(k, r) \underset{r\to\infty}{\to} N_\ell(k) \sin\left(kr - \frac{\ell\pi}{2} + \delta_\ell(k)\right) \tag{3.39}$$

where $N_\ell(k)$ is some (for now unimportant) normalization. We can expand this

$$= N_\ell(k) \frac{1}{2i} \left(\exp\left(ikr - i\frac{\ell\pi}{2}\right) e^{i\delta_\ell(k)} - \exp\left(-ikr - i\frac{\ell\pi}{2}\right) e^{-i\delta_\ell(k)}\right) \tag{3.40}$$

but we can absorb one of the phases into the normalization, and rewrite this as

$$u(k, r) \underset{r\to\infty}{\to} N'_\ell(k) \left(\exp\left(ikr - i\frac{\ell\pi}{2}\right) e^{2i\delta_\ell(k)} - \exp\left(-ikr - i\frac{\ell\pi}{2}\right)\right). \tag{3.41}$$

Define $f_\ell(k,r)$ as a solution to the radial Schrödinger equation, with the following caveats: we no longer require $f_\ell(k,0)=0$ and we impose the asympotic behavior,

$$f_\ell(k,r) \underset{r\to\infty}{\to} \exp\left(-ikr - i\frac{\ell\pi}{2}\right). \tag{3.42}$$

This is an incoming wave. Similarly we define the outgoing wave,

$$f_\ell(-k,r) \underset{r\to\infty}{\to} \exp\left(ikr - i\frac{\ell\pi}{2}\right). \tag{3.43}$$

Note that, in generally, one has to solve for $f_\ell(k,r)$ and $f_\ell(-k,r)$ independently.

We defined these as solution by specifying the asymptotic behavior as $r\to\infty$, as incoming or outgoing. But the true solution to the radial Schrödinger equation, $u_\ell(k,r)$ has a boundary condition, $u_\ell(k,0)=0$. So we write

$$\begin{aligned} u_\ell(k,r) &= N'_\ell(k)\left[f_\ell(k,r) + (-1)^{\ell+1}e^{2i\delta_\ell(k)}f_\ell(-k,r)\right], &(3.44)\\ &= N'_\ell(k)\left[f_\ell(k,r) + (-1)^{\ell+1}S_\ell(k)f_\ell(-k,r)\right], &(3.45)\end{aligned}$$

where the phase shift $\delta_\ell(k)$ is given by the boundary condition; we also see that the S-matrix in effect arises by forcing the solution to have the appropriate boundary condition at $r=0$. For $\ell>0$, we know the irregular solution or Neumann solution goes like $(kr)^{-\ell}$ as $r\to 0$, so we define the *Jost functions*

$$f_\ell(\pm k) = \lim_{r\to 0}\frac{(kr)^\ell f_\ell(\pm k,r)}{(2\ell+1)!!}. \tag{3.46}$$

Then the phase shifts, and thus the S-matrix, are given by

$$f_\ell(k) + (-1)^{\ell+1}f_\ell(-k)S_\ell(k) = 0 \tag{3.47}$$

or

$$S_\ell(k) = (-1)^\ell\frac{f_\ell(k)}{f_\ell(-k)}. \tag{3.48}$$

While this may not look like much, it allows us to derive enormous amounts of information about the S-matrix, the phase shifts, and the behavior of the scattering cross section. In particular, we consider continuation into the complex k-plane.

3.7 The S-matrix in the complex momentum plane

Although it may seem strange to the novice, it's useful to consider solutions to the radial Schrödinger equation with complex momentum p or wavenumber $k=p/\hbar$:

$$\left[-\frac{\hbar^2}{2m}\frac{d^2}{dr^2} + \frac{\hbar^2\ell(\ell+1)}{2mr^2} + V(r) - \frac{\hbar^2k^2}{2m}\right]f_\ell(-k,r) = 0$$

By taking the complex conjugate of this equation,

$$\left[-\frac{\hbar^2}{2m}\frac{d^2}{dr^2}+\frac{\hbar^2\ell(\ell+1)}{2mr^2}+V(r)-\frac{\hbar^2k^{*2}}{2m}\right]f_\ell^*(-k,r)=0 \tag{3.49}$$

we see that $f_\ell^*(-k,r)$ is a solution for complex momentum k^*. But clearly, so is $f_\ell(-k^*,r)$. The only difference is the asymptotic behavior, with

$$f_\ell^*(-k,r)\underset{r\to\infty}{\to}\exp\left(-ik^*r+i\frac{\ell\pi}{2}\right), \tag{3.50}$$

while

$$f_\ell(-k^*,r)\underset{r\to\infty}{\to}\exp\left(ik^*r-i\frac{\ell\pi}{2}\right), \tag{3.51}$$

so that

$$f_\ell^*(-k,r)=(-1)^\ell f_\ell(k^*,r). \tag{3.52}$$

This carries over to the Jost functions:

$$f_\ell^*(k)=(-1)^\ell f_\ell(-k^*). \tag{3.53}$$

From this we get two important symmetry relations:

$$S_\ell(k)S_\ell^*(k^*)=S_\ell(k)S_\ell(-k)=1. \tag{3.54}$$

Now we are in a position to interpret these complex solutions. For real values of k, $S_\ell(k)=\exp(2i\delta_\ell(k))$, which trivially has modulus one. But for complex k, the S-matrix can have modulus different from one, and can even go to zero or blow up to infinity. When $S_\ell(k)=\infty$, we call that a *pole* of the S-matrix. If you've studied complex analysis, you will remember that poles are central concepts.

By rewriting our general solution, so that

$$\begin{aligned} u_\ell(k,r) &= f_\ell(k,r)+(-1)^{\ell+1}S_\ell(k)f_\ell(-k,r) && (3.55)\\ &\propto f_\ell(-k)f_\ell(k,r)-f_\ell(k)f_\ell(-k,r) && (3.56)\end{aligned}$$

we see that when the S-matrix has a pole at k, then $f_\ell(-k)=0$ and the solution asymptotically goes like $f_\ell(-k,r)\sim\exp(+ikr)$, and that when the S-matrix has a zero at k, then $f_\ell(+k)=0$ and the solution asymptotically goes like $f_\ell(k,r)\sim\exp(-ikr)$.

So, for example, bound states have exponentially decaying solutions, that is,

$$u_\ell(r)\underset{r\to\infty}{\to}\exp(-\kappa r). \tag{3.57}$$

This corresponds to the S-matrix have a pole at $k=+i\kappa$.

Poles in the lower half plane can be written as $k=-i\kappa+\gamma$. Asymptotically these go like $\exp(+\kappa r+i\gamma r)$, that is, grow exponentially, which is unphysical but still crucial to our understanding. If $\gamma\neq 0$ these are called *resonances* and if $\gamma=0$ they are called *antibound* or *virtual states*. While resonances are not physical solutions, their influence is crucial to understand.

3.8 S-matrix poles and resonances

3.9 Application to the square well potential

For our usual attractive square well potential, that is,

$$V(r) = \begin{array}{rl} -V_0, & r \le R, \\ 0, & r > R \end{array}$$

we can compute the Jost functions for $\ell = 0$. Outside the well, we have wavenumber k, which may be complex, and a wavefunction $f_0(k,r) = \exp(-ikr)$. Inside the well, we have $f_0(k,r) = A\exp(iKr) + B\exp(-iKr)$, where $K^2 = k^2 + 2mV_0/\hbar^2$. By matching the wave function and its first derivative at $r = R$, one can solve for A and B and find that

$$f_0(k) = e^{-ikR}\left(\cos KR + i\frac{k}{K}\sin KR\right), \tag{3.58}$$

and thus

$$S_0(k) = e^{-2i\delta_0(k)} = \frac{f_0(k)}{f_0(-k)} = e^{-2ikR}\frac{K\cos KR + ik\sin KR}{K\cos KR - ik\sin KR}. \tag{3.59}$$

Note that $K(-k) = K(+k)$.

Exercise. Show you regain the analytic phase shift we found before.

Bound states are given by poles along the positive imaginary axis, that is, $k = +i\kappa$ and $K^2 = -\kappa^2 + 2mV_0/\hbar^2$. The pole in the S-matrix then is given by $K\cos KR + \kappa\sin KR = 0$, or $\kappa = -K\cot KR$.

Exercise. Compare with results for the square well from any elementary quantum text. You will have to pay attention to the boundary condition at $r = 0$.

One can also find *antibound* states, where $k = -i\kappa$, which are states which increase exponentially at large r. While unphysical, they are part of the continuation into the complex plane. For our example the solutions are given by $\kappa = +K\cot KR$.

For more general poles in the complex plane, we have to allow complex k in the lower complex plane, that is, $k = -i\epsilon + \gamma$.

3.10 Application to the δ-shell potential

After introducing the δ-shell potential in 2.5, we saw in 2.6 for the first time *resonances* or sharp peaks in the cross-section induces as the phase shift passes rapidly through $\pm\frac{\pi}{2}$. Indeed, that was my motivation in introducing an otherwise odd and not very physical potential. Now we can analyze its pole structure.

First one must get the Jost function. Much like the square well, for $r > R$, we have $f_0(k,r) = \exp(-ikr)$, while for $r < R$ we have $f_0(k,r) = A\exp(ikr) + B\exp(-ikr)$. Matching the wavefunctions at $r = R$ we have

$$A\exp(2ikR) = 1 - B.$$

By integrating the Schrödinger equation around $r = R$, we can show the Jost function is

$$f_0(k) = A + B = 1 - \frac{ik_0}{2k}\left(1 - e^{-2ikR}\right). \tag{3.60}$$

From this the S-matrix is

$$S_0(k) = \frac{f_0(k)}{f_0(-k)} = \frac{k - 2ik_0\left(1 - e^{-2ikR}\right)}{k + 2ik_0\left(1 - e^{2ikR}\right)} \tag{3.61}$$

The poles of the S-matrix are then given by

$$k = -\frac{1}{2}ik_0\left(1 - e^{2ikR}\right). \tag{3.62}$$

Breaking into real and imaginary parts, $k = \gamma + i\epsilon$,

$$\epsilon = -\frac{1}{2}k_0\left(1 - e^{-2\epsilon R}\cos(2\gamma R)\right), \tag{3.63}$$

$$\gamma = -\frac{1}{2}k_0 e^{-2\epsilon R}\sin(2\gamma R). \tag{3.64}$$

When $k_0 < 0$ and $\gamma = 0$ we regain the bound state condition (2.53), with the bound state energy $E = -\hbar^2\epsilon^2/2m$; for general poles we have to search for self-consistent solutions.

3.11 Project 3

Find the s-wave poles of the attractive square well? of the δ-shell potential?

Part II

Numerical calculations

Chapter 4

Discretizing the continuum in coordinate space

4.1 The mathematics of continuum states

When we first learn quantum mechanics, we generally work with finite, bounded states. That is, when we solve the one-dimensional Schrödinger equation,

$$\hat{H}\psi_n(x) = \left(-\frac{\hbar^2}{2m}\frac{d^2}{dx^2} + V(x)\right)\psi_n(x) = E_n\psi_n(x), \tag{4.1}$$

we first focus on solutions labeled by discrete integers $n = 1, 2, 3, \ldots$ and which have finite orthonormality relations,

$$\int_{-\infty}^{\infty} \psi_m^*(x)\psi_n(x)\,dx = \delta_{m,n} \tag{4.2}$$

where $\delta_{m,n}$ is the *Kronecker-δ* and $= 1$ if $m = n$ and $=0$ if $m \neq n$. Often we simplify this using the Dirac bra-ket notation,

$$\hat{H}|\Psi_n\rangle = E_n|\Psi_n\rangle, \tag{4.3}$$

and

$$\langle\Psi_m|\Psi_n\rangle = \delta_{m,n} \tag{4.4}$$

(If you are somehow unfamiliar with this notation, get yourself a current quantum mechanics textbook, for example Griffths or Shankar.) Even when we work in three-dimensions, we focus either on cases which have only discrete solutions, such as the three-dimensional harmonic oscillator, or, in the case of the Coulomb potential (hydrogen atom), consider only the bound states.

Continuum states, also called scattering states or unbound states, are technically more challenging, and thus are generally less emphasized in introductory

courses and texts. Consider the free particle in one-dimension, with the Hamiltonian

$$\hat{H} = -\frac{\hbar^2}{2m}\frac{d^2}{dx^2}.$$

The eigenstates are $\exp ikx$ where the wavenumber k is any real number, with energies $E(k) = \hbar^2 k^2/2m$. (We can relate the wavenumber to momentum by $p = \hbar k$.) But x can range from $-\infty$ to $+\infty$, and so any normalization integral diverges. Furthermore, on any interval of wavenumbers there are an infinite number of values of k.

The solution to the normalization problem, of course, is to generalize the Kronecker-δ to a Dirac-$\delta(x)$. Technically the Dirac-δ is not a function but a distribution or a limit function, but for simplicity it's often called the Dirac δ-function. You've probably encountered it before. It has the properties

$$\delta(x) = 0, \quad x \neq 0; \tag{4.5}$$

$$\delta(0) = \infty; \tag{4.6}$$

$$\int_a^b \delta(x)\,dx = 1 \text{ if } a < 0 < b, \quad \text{else } = 0. \tag{4.7}$$

In other words, the Dirac δ-'function' is infinitely narrow, infinitely high at $x = 0$, and has unit area. (We also deduce the units of $\delta(x)$ are 1/length, if x has units of length.)

There are several ways one can represent the Dirac δ-function. One can represent it as a limit function, i.e., an infinitely narrow Gaussian,

$$\delta(x) = \lim_{a\to 0} \sqrt{2\pi a^2}\exp\left(-\frac{x^2}{2a^2}\right) \tag{4.8}$$

or an infinitely narrow box function,

$$\delta(x) = \lim_{a\to 0} \begin{cases} \frac{1}{a}, & -\frac{a}{2} \le x \le +\frac{a}{2}, \\ 0, & |x| > \frac{a}{2} \end{cases} . \tag{4.9}$$

For our purposes, however, we want to use the Fourier representation:

$$\delta(x) = \frac{1}{2\pi}\int_{-\infty}^{\infty} e^{ikx}\,dk. \tag{4.10}$$

Then the 'normalized' eigenfunctions of the free particle are

$$\langle x|k\rangle = \phi_k(x) = \frac{1}{\sqrt{2\pi}}e^{ikx} \tag{4.11}$$

and the corresponding orthonormality relation is

$$\langle k|k'\rangle = \frac{1}{2\pi}\int_{-\infty}^{\infty} e^{-ikx}e^{ik'x}\,dx = \delta(k-k'). \tag{4.12}$$

While this is a formal generalization to continuum states, it is not very practical. In much of the rest of this book I will be describing practical methods to deal with continuum states.

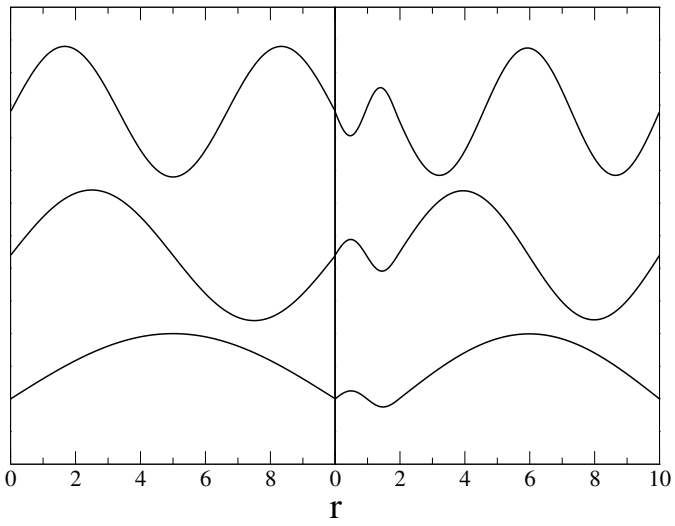

Figure 4.1: s-wave continuum wave functions in a box of length 10. Left-hand side: no potential ("free" particle). Right-hand side: attractive square well potential of radius $R = 2$, depth $V_0 = 5$.

4.2 Boxing up the continuum

So how do we deal with the troublesome infinities of continuum states? In physics and many other fields, we often solve problems by making them look like other problems we already know how to solve. We take the same strategy here: we make the continuum states look like bound states.

The simplest way is to put the problem in a box. This converts an infinite problem into a finite problem. Consider a box of size L, that is, $0 \leq x \leq L$. For free particles of mass m, the Hamiltonian is the kinetic energy operator,

$$\hat{T} = -\frac{\hbar^2}{2m}\frac{d^2}{dx^2}, \tag{4.13}$$

but with wavefunctions vanishing at the boundaries $x = 0$ and L. The eigenstates are sine functions,

$$\psi_n(x) = \sqrt{\frac{2}{L}}\sin\frac{n\pi x}{L}, \tag{4.14}$$

with energies

$$E_n = \frac{\hbar^2\pi^2 n^2}{2mL^2}. \tag{4.15}$$

These states approximate the continuum, or rather, are a subset of continuum states. Later, in section 5.1 I will discuss how to compute phase shifts in this discrete Fourier space. In almost all our methods we discuss, however, we discretize the continuum, by finding a finite subset of continuum states.

Fig. 4.1 shows the lowest continuum states in a box of size $L = 10$. The left hand side is for the "free" particle, without any potential; for the s-wave ($\ell = 0$), these are just sine functions. The right-hand side are states in the presence of an attractive square well potential of radius $R = 2$ and depth $V_0 = 5$ (and $m = \hbar = 1$). Notice that the right-hand side looks a lot like the left hand side, except for the distortions due to the presence of the attractive well.

But now we must have practical ways to calculate scattering states and their phase shifts. A straightfoward approach is to calculate on a lattice in coordinate space. That is, for a given integer N we introduce a lattice space $\Delta r = L/(N+1)$ assign $r_i = i\Delta r, i = 1, 2, 3, \ldots, N$. The radial wavefunction similarly is discretized,

$$u_i = u(r_i), i = 1, 2, 3, \ldots, N. \tag{4.16}$$

Notice that this leaves off $u_0 = u(0)$ and $u_{N+1} = u(L)$. (**Important**: This is when the vector u_i goes from $i = 1$ to $i = N$ as in Fortran. If you are using Python or C, where the default goes from $i = 0$ to $i = N - 1$, then $u_{-1} = u(x = 0) = 0$ and $u_N = u(x = L) = 0$.) Instead, we implicitly assume $u(0) = u(L) = 0$, as boundary conditions.

We want to solve the radial Schrödinger equation; to do this we need a discrete approximation to the second derivative. Fortunately this is well-known:

$$\left.\frac{d^2u(r)}{dr^2}\right|_{r=r_i} = \frac{u(r_i + \Delta r) - 2u(r_i) + u(r_i - \Delta r)}{\Delta r^2} = \frac{u_{i+1} - 2u_i + u_{i-1}}{\Delta r^2} \tag{4.17}$$

If we treat $u(r)$ as a vector $(u_1, u_2, u_3, \ldots, u_N)$ (and we should), then the second derivative is just a liinear transformation, that is, a matrix:

$$\frac{d^2}{dr^2} = \frac{1}{\Delta r^2}\begin{pmatrix} -2 & 1 & 0 & 0 & 0 & \ldots \\ 1 & -2 & 1 & 0 & 0 & \\ 0 & 1 & -2 & 1 & 0 & \\ 0 & 0 & 1 & -2 & 1 & \\ \vdots & & & & & \ddots \end{pmatrix} \tag{4.18}$$

This is very nice, but about at the boundaries? This discretization scheme says the second derivative at r_1, right next to the boundary at the origin, is

$$\frac{d^2u_1}{dr^2} = \frac{-2u_1 + u_2}{\Delta r^2}.$$

Fortuitously, we interpret this to mean that $u_0 = u(r = 0) = 0$, that is, a vanishing boundary condition. The same thing happnes for $u_{N+1} = u(L) = 0$.

You can, and should, test at this point. Using the above discretization, confirm when you diagonalize

$$-\frac{\hbar^2}{2m}\frac{d^2}{dr^2}$$

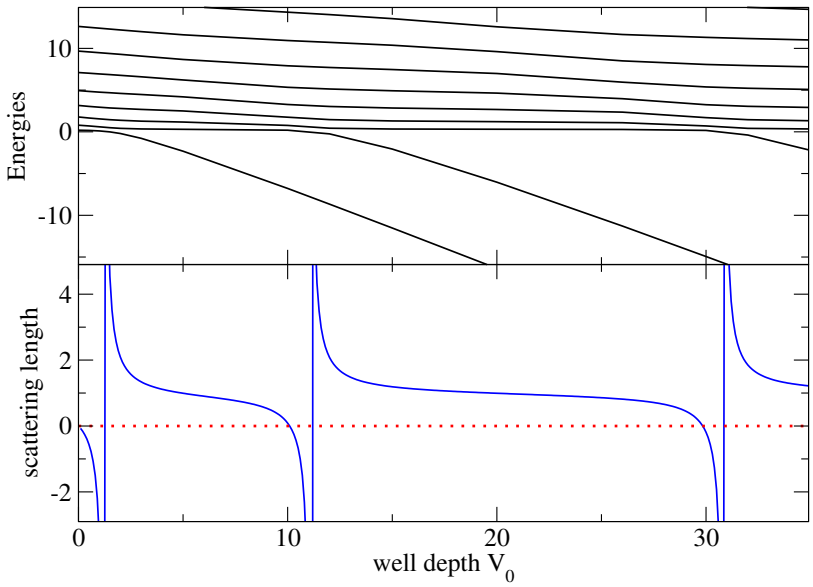

Figure 4.2: Discretization of the continuum and the rise of bound states. Here is a particle of mass $m = 1$ with $\hbar = 1$, with a wall at $L = 5$, with angular momentum $\ell = 0$, with a square well potential of radius $R = 1$ and variable depth V_0. *Top*: Lowest ten or so energies for the system as a function of well depth V_0. *Bottom*: Scattering length a as a function of V_0. The red dotted line at zero scattering length is to guide the eye.

that is, the radial kinetic energy,

$$T_{m,n} = -\frac{\hbar^2}{2m\Delta r^2}\left(\delta_{m,n+1} + \delta_{m,n-1} - 2\delta_{m,n}\right) \tag{4.19}$$

you get the expected spectrum for a particle in a box: $E_n = \hbar^2\pi^2 n^2/2mL^2$, for $n = 1, 2, 3\ldots$. The eigenfunctions should be sine functions, proportional to $\sin(n\pi r/L)$; but note, if you use an numerical eigensolver, there could be an arbitrary phase $\pm$, and it will not be normalized by an integral, that is, not by $\int_0^L u(r)^2 dr = 1$, but most likely as a vector: $\sum_{i=1}^N u_i^2 = 1$. The eigensolver doesn't know it's solving a discretized differential equation and doesn't know the 'natural' convention for the phase.

After you have confirmed you get the particle-in-a-box solutions, you can add in a potential:

$$V_{mn} = \delta_{m,n} V(r_n) \tag{4.20}$$

Let's pause here, considering first only the s-wave scattering, to solve numerically. The parameters V_0 and R define the potential. To define the discretization, you have to choose some value of L as well as N, number of lattice points. Then create the $N \times N$ matrix $H_{mn} = T_{mn} + V_{mn}$ and run through your favorite

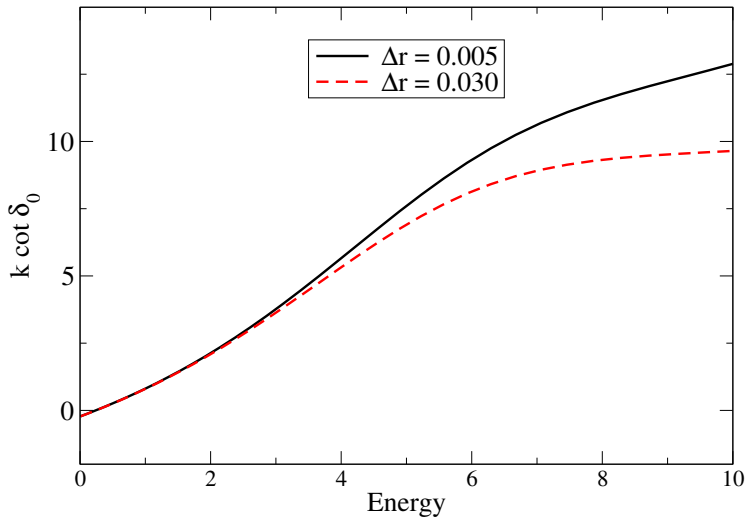

Figure 4.3: The importance of checking your discretization! A plot of $k \cot \delta_0$ for the square well with $V_0 = -1.5$, well radius $R = 1$ and $m = \hbar = 1$. Here I used a box size of 30, with 6000 and 1000 grid points to give $\Delta r = 0.005$ and 0.030, respectively.

eigensolver. You will get out a set of eigenenegies $E_i, i = 1, N$. If $E_i < 0$, it a bound state. If $E_i > 0$, it is a scattering state. In reality there are an infinite number of scattering states $u(r, E)$, but the wall at $r = L$ selects out those that vanish at $r = L$, which means $u(L, E_i) \propto \sin(k(E_i)L + \delta) = 0$.

An example of the energies is shown in Fig. (4.2), for a simple case with $m = \hbar = 1$ and wall $L = 5$ and square well radius $R = 1$. As the depth of the potential V_0 is lowered, bound states start to appear. Coinciding with each new bound state, the scattering length a goes from $-\infty$ to $+\infty$; this is known as *Levinson's theorem*. We also saw back in Fig. 2.2 that the slope of the phase shift increases and then switchs abruptly to negative. The bound state energies, that is, energies less than zero, are mostly independent of the wall distance L, but the continuum energies, those greater than zero, are quite sensitive to L.

To interpret this is somewhat subtle. Let E_i be the nth scattering state (that is, if there are n_b bound states, $n = i - n_b$, with $n \geq 1$). If there is no scattering potential, then $k(E_i)L = n\pi$, but here we must have $k(E_i)L + \delta = n\pi$, so that

$$\delta(E_i) = n\pi - \frac{\sqrt{2mE_i}}{\hbar} L. \tag{4.21}$$

Now we can compare these numerical results against the exact s-wave phase shifts from (2.14).

A note on numerics. Whenever carrying out a numerical calculation, you should investigate how sensitive your results are to your numerical parameters;

in this case, to N and to L. In principle, different choices of L merely result in different subsets of scattering states. *You should confirm this for yourself.* You should also investigate the sensitivity to your choice of Δr which is also the sensitivity to N. You should choose N such that your results do not vary much when you change N.

An example of this is given in Fig. 4.3, where I choose two different discretizations for the attractive square well with parameters $m = \hbar = 1$, well radius $R = 1$ and depth $V_0 = 1.5$. Notice the deviation occurs around an energy of 5, which corresponds to a wavenumber $k \approx 3$.

A note on ambiguities in the phase shifts. Once you start plotting phase shifts, you will notice that phase shifts can sometimes jump around. This is easily understood that one can add or subtract 2π to any phase shift and get the exact same result. If you are trying, however to fit the parameters of a potential to a set of phase shifts this can be troublesome. One option is to not plot the phase shifts but, for example $k \cot \delta$, which has no ambiguity and has the further advantage of tying into the effective range expansion of section (2.4).

Now we can easily generalize. For example, we can generalize to any local potential $V(r)$ such as a Gaussian or Woods-Saxon potential.

We can also consider higher value of orbital angular momentum ℓ. You have to add in the rotational kinetic energy term,

$$\delta_{mn} \frac{\hbar^2 \ell(\ell+1)}{2mr_n^2}.$$

To get the phase shifts, we have to use (2.4) and (2.8). Again we use the boundary condition at the wall, $u_\ell(L) = 0$ which means

$$A_\ell L j_\ell(kL) - B_\ell L n_\ell(kL) = 0. \tag{4.22}$$

Just as in the s-wave case, we numerically find a discretized continuum spectrum, E_i, taking only the positive energies. (Negative energies are still bound states.) From this we have $k_i = \sqrt{2mE_i}/\hbar$ and

$$\tan \delta_\ell(k_i) = \frac{B_\ell}{A_\ell} = \frac{j_\ell(k_i L)}{n_\ell(k_i L)}. \tag{4.23}$$

You should solve this numerically and compare to analytic phase shifts derived above.

4.3 The δ-shell potential

We can also solve the δ-shell potential numerically, although it must be handled delicately.

Check that you reproduce the analytic phase shifts, and if you did Exercise 2.8, confirm you reproduce the bound state energy.

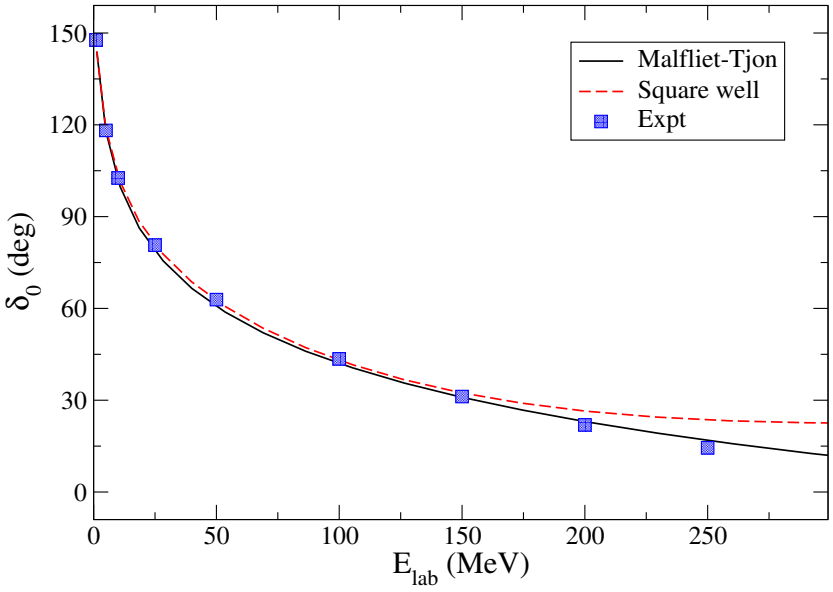

Figure 4.4: s-wave phase shifts for the Malfiiet-Tjon potential, a square well potential, and experimental $^3S_1$ phase shifts versus lab energy. See text for details.

4.3.1 A note on numerical eigensolvers

To reproduce this

4.4 Beyond the square well

Here I introduce some potentials which cannot be solved exactly but must be tackled numerically.

Malfliet-Tjon
Malfliet-Tjon is a simple approximation for for the nucleon-nucleon force:

$$V_{MT}(r) = -V_A \frac{e^{-\mu_A r}}{r} + V_R \frac{e^{-\mu_R r}}{r} \tag{4.24}$$

The original values were

$$\mu_A = 1.55\,\mathrm{fm}^{-1}, \;\; \mu_R = 3.11\,\mathrm{fm}^{-1}, \tag{4.25}$$

$$V_A = 635\,\mathrm{MeV} - \mathrm{fm}, \;\; V_R = 1458\,\mathrm{MeV} - \mathrm{fm}. \tag{4.26}$$

Fig. 4.4 shows the s-wave scattering off the Malfliet-Tjon potential against the experimental neutron-proton $^3S_1$ scattering phase shifts. (Experimental data from Wiringa, Stoks, and Schiavilla, Phys. Rev. C **51**, 38 (1995)). Here

I give the phase shifts in degrees, against the lab energy $E_{\rm lab} \approx 2 \times E_{\rm c.m.}$. (You should convince yourself why this is correct in the non-relativistic limit.) Experimentally, the bound state, the deuteron, has a binding energy of 2.2245 MeV, while in this channel the scattering length is 5.42 fm and the effective range is 1.76. The Malfiet-Tjon potential gives a deuteron binding energy of 2.40 MeV, a scattering length of 5.36 fm, and an effective range of 1.88 fm. A square well potential of radius 2 fm and depth of 36.5 MeV has a bound state energy of 2.19 MeV, a scattering length of 5.38 fm, and an effective range of 1.70 fm.

4.4.1 Finding the scattering length and effective range numerically

Because we do not have analytic expressions for general potentials, in order to find the scattering length and effective range we have to do a polynomial fit to $k \cot \delta_0$. To do this we use least-squared linear fits, a topic you likely have encountered before but which I briefly summarize here.

Given a set of N data points, $\{(x_i, y_i)\}, i = 1, N$, we want to find a function $f(x)$ which approximates y. To do this we expand $f(x)$ in some set of K basis functions $\{g_\alpha(x)\}, \alpha = 1, K$, with linear coefficients c_α, that is,

$$y \approx \sum_{\alpha=1}^{K} c_\alpha g_\alpha(x). \tag{4.27}$$

To find the best set of coefficients c_α, we minimize

$$\chi^2 = \sum_{i=1}^{N} \left(y_i - f(x_i)\right)^2 = \sum_{i=1}^{N} \left(y_i - \sum_{\alpha=1}^{K} c_\alpha g_\alpha(x_i) \right)^2 . \tag{4.28}$$

The minimum is given by

$$c_\alpha = \sum_\beta (\mathbf{A}^{-1})_{\alpha\beta} b_\beta \tag{4.29}$$

where

$$A_{\alpha\beta} = \sum_{i=1}^{N} g_\alpha(x_i) g_\beta(x_i), \tag{4.30}$$

$$b_\beta = \sum_{i=1}^{N} g_\beta(x_i) y_i. \tag{4.31}$$

For a polynomial least-squared fit, we simply choose $g_\alpha(x) = x^{2(\alpha-1)}$; one can show the $k \cot \delta$ must be an even function of k, and if you use even and odd powers of k you may not get a good fit. One should be careful to not overfit,

that is, for our purposes choose $K = 3$ (quadratic) or 4 (cubic) at most. When we do the fit, $c_0 = -1/a$ and $c_1 = 2r_{\rm eff}$.

In principle one can also extract the uncertainty in the coefficients, but that requires knowing the uncertainty in the energies, which I will try to cover later.

Chapter 5

Discretizing the continuum in Hilbert spaces

When you take a serious course in quantum mechanics, one of the first tasks is to unlearn all your erroneous notions about vectors and to learn properly about vectors spaces. In mathematics, and in mathematical physics, vectors are *not* 'magnitude plus direction;' instead a *vector* is a member of a *vector space* which satisfies certain properties. I'm presuming of course you've gone through this. Along with general, abstract vector spaces one needs to add in an inner product and you've got a *Hilbert space*, which is the basis of quantum mechanics. This is not a rigorous mathematics text, so I will just say that a Hilbert space is a vector space, that is a set of vectors $\{|a\rangle\}$, with an inner product defined. Mathematicians tend to use the notation (a, b) to denote an inner product, but we will use the physics notation of a bra-ket:

$$\langle a|b\rangle$$

which allows us to define normalization, to find the components of a vector in some basis, and all the other tasks necessary for quantum mechanical calculations.

In quantum mechanics we often use *function spaces*, where we treat functions $f(x)$ as vectors and normalize them, expand in a basis, and so on. When you first encountered function spaces they probably seemed very weird and counter-intuitive (which is why we need formal definitions of the properties of vector spaces, inner products, and so on, because then we can apply them to situations where our old intuition fails us) but by now they probably seem natural; strange how quickly we can adapt to new ideas!

One representation of the continuum are Fourier states,

$$\frac{1}{\sqrt{2\pi}} e^{ikx},$$

But we can use Hilbert spaces, specifically Hilbert function spaces, to discretize

the continuum; in particular we can use bound-state-like basis states, which makes our life easier. This is called the J-matrix method.

5.1 Phase shifts in a discrete Fourier space

Before we go on to the J-matrix method, let's calculate phase shifts in a discrete Fourier space. We work, as before, in a radial box of radius L, with normalized radial states

$$u_n(r) = \frac{\sqrt{2}}{L} \sin \frac{n\pi r}{L}. \tag{5.1}$$

The matrix elements of the radial kinetic energy are diagonal and trivial:

$$T_{mn} = \langle m|\hat{T}|n\rangle = \int_0^L u_m^*(r) \left(-\frac{\hbar^2}{2m}\frac{d^2}{dr^2}\right) u_n(r)\, dr = \delta_{m,n} \frac{\hbar^2\pi^2 n^2}{2mL^2}, \tag{5.2}$$

For the potential, $\hat{V}$, we need to take integrals,

$$V_{mn} = \langle m|\hat{V}|n\rangle = \int_0^L u_m^*(r) V(r) U_n(r)\, dr. \tag{5.3}$$

For a finite square well, we can compute this analytically:

$$V_{mn} = -V_0 \frac{2}{L} \int_0^R \sin\left(\frac{m\pi r}{L}\right) \sin\left(\frac{n\pi r}{L}\right)\, dr \tag{5.4}$$

using the trig identity $\sin a \sin b = (1/2)(\cos(a-b) - \cos(a+b))$, as well as

$$\int_0^R \cos\left(\frac{k\pi r}{L}\right)\, dr = \frac{L}{k\pi} \sin\frac{k\pi R}{L}$$

for $k \neq 0$, and $= R$ for $k = 0$. Thus, for $m \neq n$

$$V_{mn} = -V_0 \frac{1}{\pi}\left[\frac{1}{m-n}\sin\left(\frac{(m-n)\pi R}{L}\right) - \frac{1}{m+n}\sin\left(\frac{(m+n)\pi R}{L}\right)\right] \tag{5.5}$$

and on the diagonal

$$V_{nn} = -V_0\left[\frac{R}{L} - \frac{1}{2\pi n}\sin\left(\frac{2n\pi R}{L}\right)\right]. \tag{5.6}$$

Let's pause here, considering first only the s-wave scattering, to solve numerically. The parameters V_0 and R define the potential. To define the discretization, you have to choose some value of L as well as N, the maximum value of the index n labeling the sine functions. Then create the $N \times N$ matrix $H_{mn} = T_{mn} + V_{mn}$ and run through your favorite eigensolver. You will get out a set of eigenenegies $E_i, i = 1, N$. If $E_i < 0$, it a bound state. If $E_i > 0$, it is a scattering state. In reality there are an infinite number of scattering states

$u(r, E)$, but the wall at $r = L$ selects out those that vanish at $r = L$, which means $u(L, E_i) \propto \sin(k(E_i)L + \delta) = 0$.

To interpret this is somewhat subtle. Let E_i be the nth scattering state (that is, if there are n_b bound states, $n = i - n_b$). If there is no scattering potential, then $k(E_i)L = n\pi$, but here we must have $k(E_i)L + \delta = n\pi$, so that

$$\delta(E_i) = n\pi - \frac{\sqrt{2mE_i}}{\hbar}L \tag{5.7}$$

For $\ell > 0$ we need the rotational kinetic energy term,

$$T^{\rm rot}_{m,n} = \int_0^L u^*_m(r)\frac{\hbar^2\ell(\ell+1)}{2mr^2}u_n(r)\,dr. \tag{5.8}$$

For this we approximate $L \approx \infty$ and use

$$\int_0^\infty \frac{1}{x^2}\sin ax \sin bx\,dx = \frac{\pi}{2}\min(a, b). \tag{5.9}$$

While with proper massaging one can get this from MatLab or Mathematica, one can also look up this integral in a table of integrals or, as done in the appendix, use contour integrals. Then

$$T^{\rm rot}_{m,n} = \frac{\hbar^2\ell(\ell+1)\pi^2}{2mL^2}\min(m, n) \tag{5.10}$$

Then diagonalize as before

$$T_{m,n} + T^{\rm rot}_{m,n} + V_{m,n}$$

and solve for phase shifts. If you have bound states, the bound state energies should be nearly the same as your results for discretization in the box.

5.1.1 The δ-shell potential

You can also solve for the δ-shell potential. The matrix elements are analytic and straightforward. Reproduce prior results.

5.1.2 A cross-check on matrix elements

One of the prime achievements of science is to recognize humans are inevitably fallible and to develop systematic, nearly paranoid checks on our results to find those mistakes. For example, all along I have been encouraging you to compare your numerical results for the square well (and in the next subsection, the δ-shell potential).

Another test or diagnostic is to look at matrix elements of a potential $V(r)$ in a basis. How can we know when we have included enough states, that is, gone up to high enough n? One way is a straightforward sum rule. If $V(r)$ is of a single sign, that is, is always negative or *always* positive, then it is should be

obvious that $V_{n,n}$ is always of the same sign too. Then, by using a completeness relation, we arrive at

$$\int_0^\infty V(r)\,dr = \sum_n V_{n,n}. \tag{5.11}$$

In cases where we know $V_{n,n}$ is always of a fixed sign, then we know that $\int_0^\infty V(r)\,dr$ will always be a bound, either upper or lower, on a finite sum $\sum_n^{N_{\max}} V_{n,n}$.

NOTE: I am not sure this is completely correct. Still trying to work out.

Exercise. For a spherical square well of radius R and depth $-V_0$, $\int_0^\infty V(r)\,dr = -V_0 R$. Plot this against the running sum of $V_{n,n}$, using Eq. (5.6).

5.2 The J-matrix method

In general, the J-matrix method is when the kinetic energy T is tridiagonal in the basis, even if the basis states are "bound." There are two main J-matrix regimes, the harmonic oscillator basis and the Laguerre basis, but any basis for which T is tridiagonal would work.

The basic idea is very similar to that for the continuum discretized in coordinate space: in a given basis, we have

$$\mathbf{H} \approx \begin{pmatrix} \mathbf{T}+\mathbf{V} & 0 \\ 0 & \mathbf{T} \end{pmatrix}, \tag{5.12}$$

that is, for some finite set of basis states we have both the kinetic and potential energies, but beyond that set only the kinetic energy is important. If the kinetic energy is tridiagonal, then we can solve for the vectors by a recursion relation.

We will take a simplified version of J-matrix theory, however, inspired by our earlier results. We will simpy cut off at some maximum basis N. Diagonalizing, the continuum is discretized, and if

$$\mathbf{H}\vec{v} = E\vec{v} = \frac{\hbar^2 k^2}{2m}\vec{v}, \tag{5.13}$$

then it implies that $v_{N+1} = 0$. From this we can extract the phase shift.

This idea is illustrated in Fig. 5.1. This sample calculation shows a calculation in some basis–here a harmonic oscillator basis, though that is not important–and by truncated to some $N_{\max}$, forcing the wave function in the Hilbert space to have a node (a zero) at $N_{\max}+1$, where the red dashed line is. This works the same in discretized coordinate space (but I have yet to add the corresponding figure).

Specifically, let $\{\phi_i(r)\}, i = 1, N$ be our radial basis states. Because we assume bound states, they have the convenient orthonormality condition,

$$\int_0^\infty \phi_i^*(r)\phi_j(r)\,dr = \delta_{ij}.$$

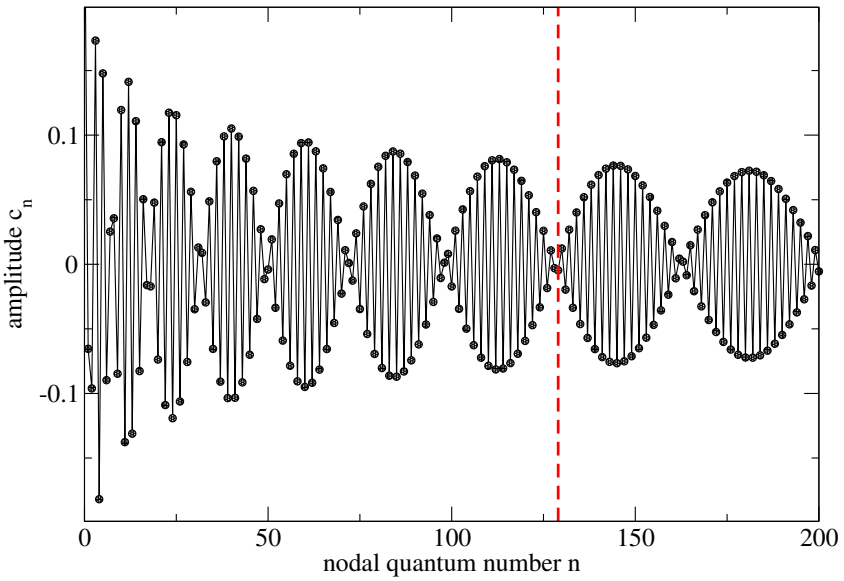

Figure 5.1: An illustration of the simplified J-matrix method. An implicit "wall" (dashed red line) is inserted, so that all solutions must have a zero (node) at the wall. The wave function actually continues on, as shown, but we only calculate the part to the left of the wall.

Then at a given eigenenergy E which corresponds to a wavenumber $k = \sqrt{2mE}/\hbar$, we expand

$$u(E,r) = \sum_i v_i(E)\phi_i(r) \tag{5.14}$$

Then the boundary condition is that $v_{N+1} = 0$. But we know that where there is only kinetic energy,

$$u(E,r) \to C\left(rj_\ell(kr)\cos\delta - rn_\ell(kr)\sin\delta\right) \tag{5.15}$$

where $V(r) = 0$. As the coefficient $v_{N+1} = 0$, we must have the orthogonality conditions

$$\int_0^\infty \phi_{N+1}(r)\left(rj_\ell(kr)\cos\delta - rn_\ell(kr)\sin\delta\right)dr = 0, \tag{5.16}$$

or

$$\tan\delta_\ell = \frac{\int_0^\infty \phi^*_{N+1}(r)j_\ell(kr)r\,dr}{\int_0^\infty \phi^*_{N+1}(r)n_\ell(kr)r\,dr}. \tag{5.17}$$

A subtle but important condition here is that $\phi_{N+1}(r)$ is vanishingly small in the region where $V(r)$ is nonzero. Fortunately our cases satisfy that.

In this basis, the matrix elements of the potential are

$$V^{(\ell)}_{n',n} = \int_0^\infty \phi^*_{n',\ell}(r)V(r)\phi_{n,\ell}(r)\,dr. \tag{5.18}$$

5.3 Harmonic oscillator basis

For much of this text we will focus on using a basis of spherical (3-dimensional) harmonic oscillator states. The full wave function is

$$\psi_{n\ell m}(r,\theta,\phi) = \frac{u_{n\ell}(r)}{r}Y_{\ell m}(\theta,\phi),$$

with ℓ the orbital angular momentum as usual and $n = 0, 1, 2, \ldots$ counts the number of nodes in the radial wave function $u(r)$ and is called the *(radial) nodal quantum number*. An alternate quantum number is $N = 2n + \ell$, the *principal quantum number*, as the energy for the harmonic oscillator Hamiltonian is $E = (N + 3/2)\hbar\omega$. The appendix describes their construction in more detail.

Fig. 5.2 shows s-wave ($\ell = 0$) harmonic oscillator for $n = 0, 100, 300$, and demonstrates how for large n the wavefunctions become almost oscillatory. They are also bounded, and we see empirically the wave functions fall off rapidly for $r > 2\sqrt{n}b$. Nonetheless we can expand Bessel and Neumann functions in terms of harmonic oscillator wave functions. Given the expansion

$$rj_\ell(kr) = \sum_{n=0} c_n\, u_{n,\ell}(r),$$

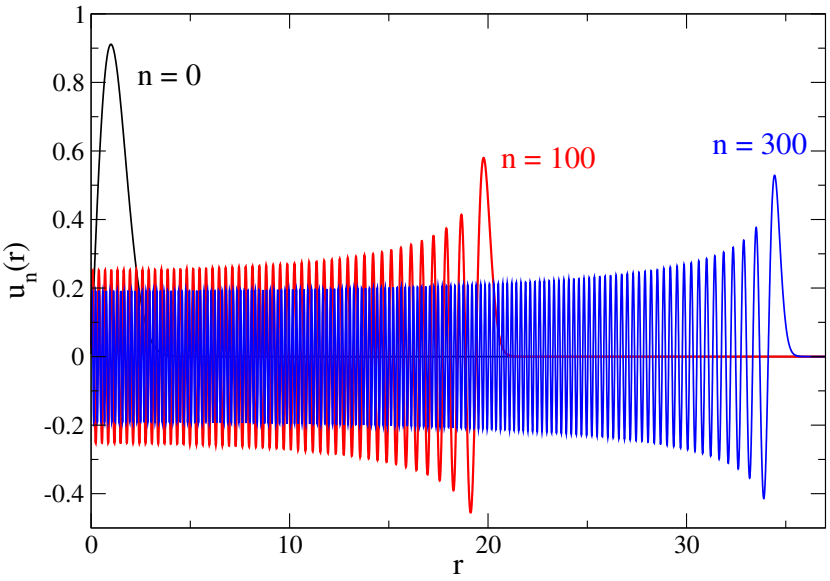

Figure 5.2: Radial spherical harmonic oscillator wavefunctions $u_n(r)$ for $n = 0, 100, 300$, with length parameter $b = 1$.

Fig. 5.3 shows the coefficients c_n for $\ell = 0$, $k = 1$, $b = 1$. You can see in this case the coefficients vanish or become very small for some values of n, illustrating the basic idea of our simplified J-matrix method.

A very useful and lucid reference is Shirokov, Mazur, Mazur, and Vary, Phys. Rev. C **94**, 064320 (2016), also arXiv:1608.05885. Note, however, some differences: I express everything in terms of the radial nodal quantum number n while Shirokov *et al.* use the principal quantum number $N = 2n+\ell$, I express my results primarily in terms of the length parameter $b = \sqrt{\hbar/m\omega}$ while Shirokov *et al.* use $\hbar\omega$, and finally and of most concern, there is a phase factor $(-1)^n$ between their radial wavefunctions $u_{n\ell}(r)$ and mine (to be further investigated).

In the harmonic oscillator basis, the matrix elements of the kinetic energy are analytic and simple–and tridiagonal, which is the whole point of the J-matrix method:

$$T^{(\ell)}_{n,n} = \frac{1}{2M}\left\langle n,\ell\left|\hat{p}^2\right|n,\ell\right\rangle = \frac{\hbar^2}{2Mb^2}(2n+\ell+3/2), \tag{5.19}$$

$$T^{(\ell)}_{n+1,n} = \frac{1}{2M}\left\langle n+1,\ell\left|\hat{p}^2\right|n,\ell\right\rangle = \frac{\hbar^2}{2Mb^2}\sqrt{(n+1)(n+\ell+3/2)}. \tag{5.20}$$

Note that $\hbar^2/(2Mb^2) = \hbar\omega$.

As an exercise, diagonalize $\mathbf{T}$ for $\ell = 0$ for some large maximum n. What does the spectrum look like? What about for $\ell > 0$? Note that in this representation, $\mathbf{T}^{(\ell)}$ includes *all* of the kinetic energy, both the 'radial' and the 'centrifugal' parts.

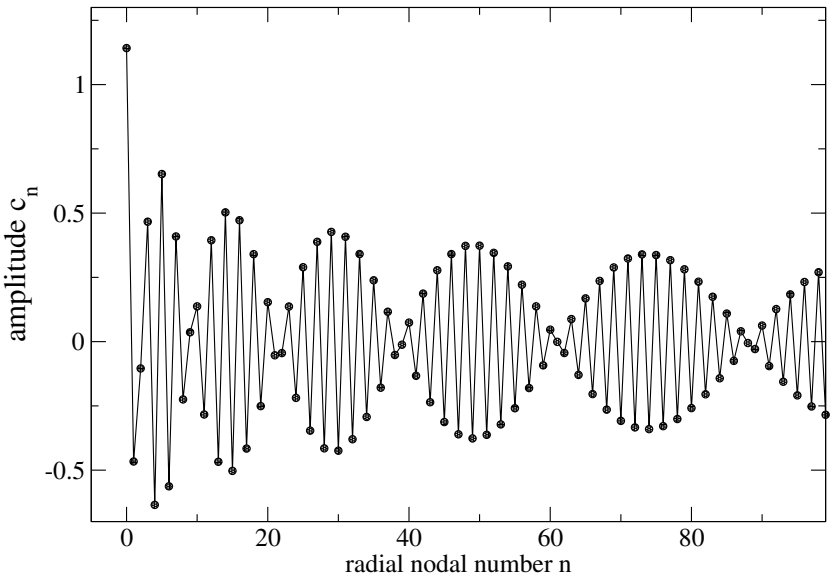

Figure 5.3: Expansion of s-wave spherical Bessel function $j_0(kr)$, with $k = 1$, into spherical harmonic oscillator basis functions with length parameter $b = 1$. The line is to guide the eye.

Exercise. Diagonalize $\mathbf{T}$ for some ℓ (always start with $\ell = 0$) and find the eigenenergies and write the eigenvector components to a file. Choose some solution and deduce $k = \sqrt{2mE}/\hbar$. Decompose $j_\ell(kr)$ into harmonic oscillator components as in Fig. 5.3. Overlay the two on a graph; they should be the same, except for some overall normalization, including possibly a phase.

Shirokov *et al.* find analytic solutions (which I have to check): *To be added.*

We should, however, be able to numerically compute the phase shifts and matrix elements using (5.17), with numerical quadrature. Appendix B discusses in some detail the radial wave functions, which can be computed using the recursion relation (B.21) starting from (B.29), (B.30). I recommend starting with integrals with Boole's rule, but then shifting to Gauss-Hermite quadrature. To check you are using an appropriate grid for either, *always* check in advance the orthonomality condition is numerically satsified.

Fig. 5.4 demonstrates the limitation of the J-matrix method, namely that in a Hilbert space the potential may not be very "localized." Here I compute the diagonal s-wave matrix elements $V_{n,n} = \langle \ell = 0, n|\hat{V}|\ell = 0, n\rangle$ as well as the off-diagonal $V_{0,n}$, for a square barrier with height 1 and with radius of 0.25 $\times b$, where b is the oscillator length parameter. We see the matrix element do not complete vanish even as far out as $n = 400$, and going to 800 does not significantly change the situation. To some extent this is a worse-case scenario.

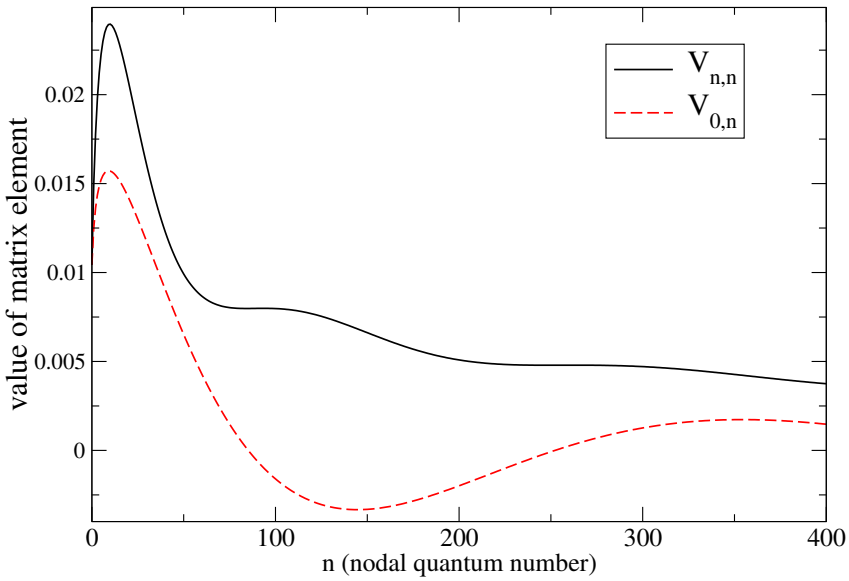

Figure 5.4: s-wave matrix elements for a square barrier of radius 0.25 and unit height, in a harmonic oscillator basis with length parameter $b = 1$.

For a radius of $1 \times b$, the central peak is much sharper and higher, so the error is smaller. Nonetheless one has to make an approximation by truncating the potential at some maximum n. You should *always* do a careful study, through plots such as this, as well as checking the dependence on the cutoff in n in the representation of the potential.

5.3.1 A toy model

For a simple toy model with one parameter, let $V_{mn} = 0$ except $V_{00} = -\bar{V}$, that is, a single point. Find the phase shifts numerically (later, using the theory of orthogonal polynomials, we'll try to find them 'analytically'). Track how bound states (with energy < 0) enter as you increase $\bar{V}$.

5.4 Laguerre basis

Chapter 6

Integral relations

Here I derive an interesting integral relation. I consider simple two-body scattering in a single channel, so that the scattering solution for angular momentum ℓ is given by the radial Schrödinger equation,

$$-\frac{\hbar^2}{2m}\frac{d^2}{dr^2}u(r)+\left(\frac{\hbar^2\ell(\ell+1)}{2mr^2}+V(r)\right)u(r)=Eu(r)=\frac{\hbar^2k^2}{2m}u(r). \tag{6.1}$$

If we leave off the potential $V(r)$ the free solution is $u_{\rm free}(r)=rj_\ell(kr)$. We can pair up the two differential equations, after multiplying through by $-2m/\hbar^2$:

$$\frac{d^2u(r)}{dr^2}+\left(k^2-\frac{\ell(\ell+1)}{r^2}-\frac{2m}{\hbar^2}V(r)\right)u(r)=0, \tag{6.2}$$

$$\frac{d^2u_{\rm free}(r)}{dr^2}+\left(k^2-\frac{\ell(\ell+1)}{r^2}\right)u_{\rm free}(r)=0 \tag{6.3}$$

Now multiply (6.2) by $u_{\rm free}(r)$ on the left, and (6.3) by $u(r)$,

$$u_{\rm free}\left[\frac{d^2u(r)}{dr^2}+\left(k^2-\frac{\ell(\ell+1)}{r^2}-\frac{2m}{\hbar^2}V(r)\right)u(r)=0\right],$$
$$u(r)\left[\frac{d^2u_{\rm free}(r)}{dr^2}+\left(k^2-\frac{\ell(\ell+1)}{r^2}\right)u_{\rm free}(r)=0\right]$$

and take the difference to get

$$\begin{aligned}-u_{\rm free}(r)\frac{2m}{\hbar^2}V(r)u(r) &= u(r)\tfrac{d^2}{dr^2}u_{\rm free}(r)-u_{\rm free}(r)\tfrac{d^2}{dr^2}u(r)\\ &= \tfrac{d}{dr}\left[u(r)\tfrac{d}{dr}u_{\rm free}(r)-u_{\rm free}(r)\tfrac{d}{dr}u(r)\right]\end{aligned} \tag{6.4}$$

Next integrate

$$-\frac{2m}{\hbar^2}\int_0^\infty u_{\rm free}(r)V(r)u(r)dr=\left[u(r)\frac{d}{dr}u_{\rm free}(r)-u_{\rm free}(r)\frac{d}{dr}u(r)\right]\Bigg|_{r=0}^{r=\infty} \tag{6.5}$$

To evaluate the righthand side, we note that both $u(0) = u_{\text{free}}(0) = 0$, and asymptotically

$$u_{\text{free}}(r) \underset{r\to\infty}{=} \frac{1}{k}\sin\left(kr - \frac{\ell}{2}\pi\right), \tag{6.6}$$

$$u(r) \underset{r\to\infty}{=} \frac{1}{k}\sin\left(kr - \frac{\ell}{2}\pi + \delta\right). \tag{6.7}$$

From this we can show

$$u(r)\frac{d}{dr}u_{\text{free}}(r) - u_{\text{free}}(r)\frac{d}{dr}u(r) \underset{r\to\infty}{=} \frac{\sin\delta}{k}. \tag{6.8}$$

Putting it all together

$$\sin\delta = -\frac{2m}{\hbar^2}k\int_0^\infty u_{\text{free}}(r)V(r)u(r)dr. \tag{6.9}$$

The beauty of this equation is that it only depends upon $u(r)$ where $V(r) \neq 0$, that is, is an integral over the "interior" of the wavefunction.

Clearly we can do this in a discrete space, at least for a two-particle system. The challenge is to carry this out for a many-body system.

Chapter 7

Direct capture and other reactions

Up until this point, we have been concerned with scattering. Now we want to shift gears and look at so-called direct reactions, such as the neutron capture reaction

$$^3\mathrm{He} + n \rightarrow ^4\mathrm{He} + \gamma.$$

This shift requires a significant change in our focus. The key idea in scattering is the change in the wave functions at large distance from the interaction region, parameterized by the phase shift or the S-matrix, with no need for knowledge of the amplitude of wave functions. As I'll discuss in more detail, capture reactions are very different: we need overlap integrals which encompass the interaction region (although as I'll show, for low energy the integrands can be maximum far outside the interaction region) and getting the amplitude right is critical.

Direct reactions are contrasted with *compound reactions*. The primary difference between direct reactions and compound reactions is that direct reactions generally go to a single, "simple" state, which compound reactions involve many, complex states. I will expand this definition later.

For now I will focus on reactions involving neutrons. Reactions involving protons and other charged projectiles are extremely important, perhaps even more so than neutrons, but the Coulomb interaction adds complexity.

In order to develop the formalism for direct reactions, let's take things step by step:

- First, we begin with γ-decay, that is, bound-state to bound-state transitions: $A^* \rightarrow A + \gamma$..
- Second, look at the reverse: photoexcitation to a bound state: $A+\gamma \rightarrow A^*$;
- Finally, look at capture and photo-disintegration, which involve scattering states: $b + c \rightarrow A + \gamma$ and $A + \gamma \rightarrow b + c$

All of these start with *Fermi's golden rule* (although it was originally derived by Dirac) for the rate from some initial state i with wave function $|\Psi_i\rangle$ to some final state f with wave function $|\Psi_f\rangle$:

$$R(i \to f) = \frac{2\pi}{\hbar} \left| \langle \Psi_f \left| \hat{H}_{\rm int} \right| \Psi_i \rangle \right|^2 \frac{dn_f}{dE}, \tag{7.1}$$

where $\hat{H}_{\rm int}$ is the interaction Hamiltonian with a sinusoidal time dependence that drives the change, that is, one assumes $|\Psi_i\rangle$ and $|\Psi_f\rangle$ are eigenstates of some static Hamiltonian $\hat{H}_0$, and the entire system evolves under

$$\hat{H}_0 + \sin(\omega t)\hat{H}_{\rm int}.$$

Finally, $\frac{dn_f}{dE}$ is the density of final states in an energy interval. As we'll see, this is often a Dirac-δ function. Fermi's golden rule is derived in most quantum textbooks in time-dependent perturbation theory, and in fact is the primary result for time-dependent perturbation theory. You should take careful note that this rate does indeed have dimensions of time^{-1}–one should *always* use dimensional analysis to check one's understanding.

Rather than simply writing down the results, let's take apart each of the pieces:

1. One needs an initial $|\Psi_i\rangle$ and a final $|\Psi_f\rangle$ wave function, both of which need to be appropriately normalized, which I discuss in detail below (or above).

2. We need an interaction operator. In the kinds of transitions discussed here, they are electromagnetic transitions. To conceptualize the process, imagine, for example, a dipole electric field oscillating with frequency ω, which corresponds to electric dipole photons of energy $\hbar\omega$.

3. We need a density of final states, $\frac{dn_f}{dE}$

4. Although it's not explicitly stated in Eq. (7.1), such transitions almost always involve a transfer and thus change of angular momentum, which must be handled properly.

5. Finally, to compute cross sections, we need an initial flux.

In the following sections, I discuss each of these in turn, followed with applications.

7.1 The headache of normalization

In our initial applications, we consider a simple model of *potential capture*, that is, modeling capture of a particle to a many-body system by a simple capture reaction in a potential. In that case the transition probability is

$$\left| \langle \psi_b | \hat{\mathcal{O}} | \psi(k) \rangle \right|^2 = \int_0^\infty u_b^*(r)\, \hat{\mathcal{O}}(r)\, u_{\rm scatt}(k, r)\, dr \tag{7.2}$$

In a section below [to be written] I will detail some possibile transition operators $\hat{\mathcal{O}}(r)$. A simple example of one is the electric dipole operator, which is just r times some constants.

This integral (7.2) may look intimidating, as the range of integral is formally from zero to infinity. Fortunately, while the scattering wave function $u_{\rm scatt}$ is doggedly nonzero even as we run endlessly towards but never reaching infinity, the integral itself is in a practical sense bound. This is because the bound state wave function $u_b(r)$ *does* fade away as $r \to \infty$.

The biggest issue reminaing is normalization. Under the Born interpretation, the square of the wavefunction is a probability or a probability density. Indeed, much of basic quantum mechanics involves learning how to transform a wave function into the appropriate representation, in which the answer is a probabilty which is just the square of the wave function–in that representation. The statement that a wave function is *normalized* is really just saying the probabilities *must* sum to one.

The bound state is easily and rigorously normalized,

$$\int_0^\infty |u_b(r)|^2 \, dr = 1. \tag{7.3}$$

You must still pay attention in numerical calculations. All numerical eigensolvers will normalize a discretized wave function u_i by

$$\sum_i |u_i|^2 = 1,$$

but (7.3) is for a uniform grid on r

$$\sum_i |u_i|^2 \, \Delta r \approx 1, \tag{7.4}$$

(the $\approx$ is because depending on the quadrature algorithm, for example trapezoidal rule versus Simpson's rule versus Boole's rule, you can get slight variations). As long as your box size is large enough, however, so that the bound state is not "crowded," the normalization should then be fixed.

Exercise 7.1. Using a code with a uniform discretization in r and a fixed box size L, solve for any wave function with N points and with $4N$ points, and plot both vectors. You should get something like [insert figure here]. If you multiple both wave functions by $1/\sqrt{\Delta r}$ they should lie nearly on top of each other. Also note that your numerical wave functions may differ by an arbitrary phase of ± 1, which has no physical meaning.

As discussed in Chapter 4, the normalization of continuum / scattering states is trickier. Our general strategy has been to take a finite space and treat continuum states like bound states. The problem that arises is the normalization then depends strongly on the box size L. For example, suppose we had a free particle,

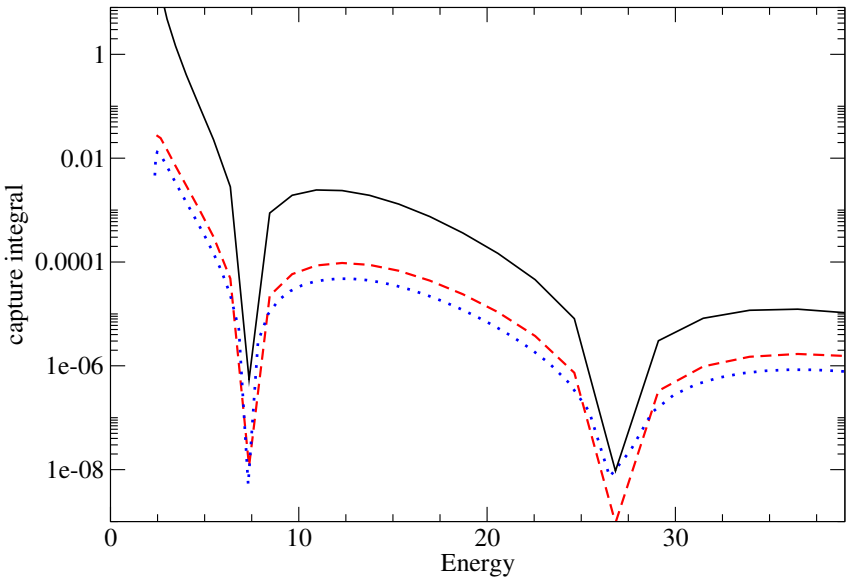

Figure 7.1: Dependence on capture integral on normalization. Square well with $m = \hbar = R = 1$, $V_0 = 5$, for two box sizes, $L = 10$ and 20. Black line is normalized to the continuum limit, while red and blue lines are normalized like bound states.

with a solution $C \sin kr$. If we follow our practice so far and put the system in a spherical box of radius L, then the normalization coefficient $C = \sqrt{2/L}$ and the transition probability (7.2) is proportional to L^{-1}. Later one we will see this is fixed by considering the flux.

It gets worse when we consider a scattering state in a potential. Although in a box of size L our instinct is to normalize as in (7.3), in fact in the limit as $L \to \infty$ the proper normalization is

$$\int_0^\infty u^*(k', r)\, u(k, r)\, dr = 2\pi\delta(k' - k). \tag{7.5}$$

The way we handle this is to realize that the integral in (7.5) is dominated by contributions far away from the potential, that is, we want

$$u(k, r) \underset{r\to\infty}{\to} \sin(kr + \delta) \tag{7.6}$$

(I am worried about a factor of k here...) So in order to take care of this, when we solving for any scattering state, we write

$$u(k, r) \underset{r\to\infty}{\to} C \sin(kr + \delta) \tag{7.7}$$

where C is the amplitude of the tail of the wave function and is related (I think) to the *asymptotic normalization coefficient* which I hope to discuss more later.

How to find the amplitude C? There are two ways. The second, which I will pick up in a separate chapter, is to use the Lippmann-Schwinger equation, where one can explicitly *start* with a correctly normalized asymptotic wave function. More about that later.

The first method, however, is to numerically find C. Previously we found the phase shift by finding an amplitude in the wave function which is zero. We have no such luck here. Instead we start from Eq. (2.4), which is true if we are outside the interaction region:

$$u_\ell(r) = A_\ell\, r j_\ell(kr) - B_\ell\, r n_\ell(kr).$$

Here is my proposed algorithm; there may be better: choose some set of $N_{\rm fit}$ grid points $\{r_i\}$, *outside the interaction region*, for example, the *last* 100 points on the grid, and the numerical wavefunction values $\{u_i\}$ at those points. We can now do a linear least-squares fit to A_ℓ and B_ℓ. For this you need to know the wave number $k = \sqrt{2ME}/hbar$. Form the 2×2 matrix $\mathbf{M}$, with

$$M_{11} = \sum_i r_i^2 j_\ell(kr_i)^2, \tag{7.8}$$

$$M_{12} = M_{21} = \sum_i r_i^2 j_\ell(kr_i) n_\ell(kr_i), \tag{7.9}$$

$$M_{22} = \sum_i r_i^2 n_\ell(kr_i)^2, \tag{7.10}$$

and the vector $\vec{b}$,

$$b_1 = \sum_i r_i j_\ell(kr_i) u_i, \;\; b_2 = \sum_i r_i n_\ell(kr_i) u_i, \tag{7.11}$$

Then

$$\begin{pmatrix} A_\ell \\ B_\ell \end{pmatrix} = \mathbf{M}^{-1}\vec{b} \tag{7.12}$$

or

$$A_\ell = \frac{1}{\det \mathbf{M}} \left(M_{22} b_1 - M_{12} b_2 \right), \tag{7.13}$$

$$B_\ell = \frac{1}{\det \mathbf{M}} \left(-M_{21} b_1 + M_{11} b_2 \right). \tag{7.14}$$

Then $C = \sqrt{A_\ell^2 + B_\ell^2}$. You can also find $\delta_\ell = \tan^{-1} \frac{B_\ell}{A_\ell}$. In fact, it's a very good and highly recommended cross-check that the phase shifts you get out of this fit are the same, or at least very similar to, those you found from the boundary condition. (You might very well ask: why not use this method from the start to determine the phase shift? It does work, but, the boundary condition is more elegant and, in my experience, more accurate.)

(**Please note I am still working on these notes and so there are likely some errors of detail !**)

7.2 Electromagnetic operators

I am focusing on transitions mediated by electromagnetism. Towards this end we need to develop the operators for electromagnetic transitions. I will not do a full development of the operators. For useful references see Blatt and Weisskopf, *Theoretical Nuclear Physics*, Roy and Nigam, *Nuclear Physics*, or the text I will most heavily rely upon, Brussaard and Glaudemans, *Shell-model applications in nuclear spectroscopy*. The latter has the most modern development, but is difficult to find. Blatt and Weisskopf, although old (1952), is readily available as a Dover edition. See also Bohr and Mottelson, Volume I, Appendix 3C. I also recommend deForest and Walecka, Adv. Phys. **15**, 1 (1966), which gives a more general and powerful point of view.

For a quick review: photons have intrinsic angular momentum or 'spin' of $1\hbar$, which in principle means they could have three components. In practice, however, because they are massless, real photons have only two components. We talk about these as being two different polarization states, but we also talk about *transverse electric* and *transverse magnetic* modes. I won't review where that terminology comes from, but only note that we retain it in talking about transitions: *electric* transitions and *magnetic* transition, and their corresponding operators. (Let me comment that when one goes away from massless photons, for example for weak transitions mediated by massive vector bosons, or when talking about electron scattering when one has 'virtual' photons "off the mass shell," then a third class of operators arises, the so-called longitudinal operators. In fact, in my development below we use longitudinal operators, but they are simply related to electric operators by Siegert's theorem in the long wavelength limit.)

Because we are working in a framework with good angular momentum, we have to worry about the angular momentum, λ of the electromagnetic radiation. Electric transitions carry parity $\pi = (-1)^\lambda$, while magnetic transitions carry parity $\pi = (-1)^{\lambda+1}$. Hence electric dipole, or E1, magnetic quadrupole, or M2, and electric octupole, or E3, all carry away parity -1, while magnetic dipole (M1), electric quadrupole (E2), and magnetic octupole (M3), all carry away parity +1. Because real photons have spin 1, we cannot have monopole, E0 or M0, radiation. Although I discuss general formalism, the most important transition operators for direct reactions are E1, M1, and E2. The reason is the long-wavelength limit. The highest the angular momentum, the more "wrinkled" the wave function is, but most radiation, even gamma rays, have wavelengths much larger than the nucleus, and so can only resolve and couple to the grossest features of the nucleus. We will see this falls out of the formalism.

Although I am treating the nucleus nonrelativistically, special relativity plays a central role in electromagnetism. Maxwell's classical electromagnetic equations assume a coupling between the electromagnetic Lorentz 4-potential A_μ, $\mu = 0, 1, 2, 3$ and the Lorentz 4-current of the nucleons, J_μ:

$$\hat{H}_{\rm int} = -\int J^\mu A_\mu \, d^3r. \tag{7.15}$$

The nuclear four-vector (ignoring factors of the speed of light c),

$$J_\mu = \left(\rho, \vec{j}\right) \tag{7.16}$$

where the nuclear charge density is

$$\rho(\vec{r}) = \sum_{i=1}^{A} e_i \delta^{(3)}\left(\vec{r} - \vec{r}_i\right) \tag{7.17}$$

where e_i is the charge of the ith nucleon (+1 for protons, 0 for neutrons). The nuclear electromagnetic current has two contributions, that due to the motion of the nucleons, and that from their magnetic moments:

$$\vec{j}(\vec{r}) = \sum_i e_i \frac{\vec{v}_i \delta^{(3)}\left(\vec{r} - \vec{r}_i\right) + \delta^{(3)}\left(\vec{r} - \vec{r}_i\right)\vec{v}_i}{2} + \mu_i \vec{\nabla} \times \vec{s}_i \left(\vec{r} - \vec{r}_i\right), \tag{7.18}$$

where s_i is the spin of the ith nucleon, v_i the velocity, and μ_i is the magnetic moment,

$$\mu_i = \frac{e\hbar}{2M_N} g_i \tag{7.19}$$

with g_i the spin g-factor, which has values X and Y for protons and neutrons, respectively. Of course, this assumes point nucleons, which is clearly wrong, but you can find corrections in other texts.

The other ingredient, the electromagnetic 4-current, also can be divided up:

$$A_\mu = (\Phi, \vec{A}) \tag{7.20}$$

with Φ the electric potential and $\vec{A}$ the vector potential. Because the magnetic field is the curl of the vector potential, we have the freedom (and the curse) to choose a particular gauge. Dealing with real photons, a natural choice is the transverse gauge condition, $\vec{\nabla} \cdot \vec{A} = 0$. In Fourier, that is, momentum space, this becomes

$$\vec{q} \cdot \vec{A} = 0, \tag{7.21}$$

where $\vec{q}$ is the *momentum transfer* carried by the photon. If we choose $\vec{q}$ to be along the z-axis, then $A_z = 0$, and hence we have, as mentioned earlier, only free two component, A_x and A_y, or some other linear combination. A particularly useful linear combination are the *transverse electric* and *magnetic* components. I won't derive these, but simply state them in multipole expansions, which depend upon q (the wave number for momentum transfer), angular momentum λ and z-component μ:

$$\mathcal{T}(E\lambda, \mu; q) = -i\frac{(2\lambda+1)!!}{q^{\lambda+1}(\lambda+1)} \int \vec{j}(\vec{r}) \cdot \vec{\nabla} \times \left(\vec{r} \times \vec{\nabla}\right) \left(j_\lambda(qr) Y_{\lambda\mu}(\hat{r})\right) d^3r, \tag{7.22}$$

$$\mathcal{T}(M\lambda, \mu; q) = -\frac{(2\lambda+1)!!}{q^{\lambda}(\lambda+1)} \int \vec{j}(\vec{r}) \cdot \left(\vec{r} \times \vec{\nabla}\right) \left(j_\lambda(qr) Y_{\lambda\mu}(\hat{r})\right) d^3r. \tag{7.23}$$

7.3 Angular momentum algebra

7.4 Putting it all together: Flux and density of final states

7.5 Applications and examples

7.5.1 Application: Gamma transitions

7.5.2 Application: Photoemission of neutron

Here let's consider a very specific example of the deuteron. To begin with, let's consider a toy model for the deuteron bound-state wave function: let $u_b(r) = 2\kappa^{3/2} r \exp(-\kappa r)$, where $\kappa = \sqrt{2\mu|E_b|}/\hbar$, with $\mu = M_N/2$ is the reduced mass, and $E_b \approx -2.2$ MeV is the deuteron binding energy. This toy wave function is wrong in the interior, but has the correct asymptotic fall off.

More generally, if we consider E1 capture, the operator is approximation r, and the capture integral is

$$\int_0^\infty dr\, r^2 2\kappa^{3/2} \exp(-\kappa r) \sin kr = 4k\kappa^{3/2} \frac{3\kappa^2 - k^2}{(\kappa^2 + k^2)^3}. \tag{7.24}$$

If we look at the integrand in some detail, we learn an important lesson. For small enough k, $\sin kr \approx kr$ and the integral becomes

$$\sim k \int_0^\infty dr\, r^3 \exp(-\kappa r)$$

The integrand is peaked around $r = 3/\kappa$. For the deuteron, this is around 13 fm, far outside the nucleus! Furthermore, the integrand has a long tail, which means one has to integrate far out for small k.

7.5.3 Application: Direct capture of neutron

7.6 The Lippmann-Schwinger equation, numerically

Another way to write the Lippmann-Schwinger equation is

$$|\Psi\rangle = |\Psi_0\rangle + \frac{1}{E - \hat{H} + i\epsilon} \hat{V} |\Psi_0\rangle, \tag{7.25}$$

where $\hat{H} = \hat{H}_0 + \hat{V}$, with H_0 typically the kinetic energy, $\hat{H}_0|\Psi_0\rangle = E|\Psi_0\rangle$, and $\hat{H}|\Psi\rangle = E|\Psi\rangle$.

We can do this numerically, by adapting the code we used to solve for scattering.

The advantage of this formulation of the Lippmann-Schwinger equation is twofold. First, we get automatically the correct normalization if we choose $|\Psi_0\rangle$ as a free solution with the correct normalization. Second, this formulation is amenable to the Lanczos algorithm, making it tractable.

Part III

Scattering and capture with Coulomb

Appendix A

Sturm-Liouville differential equations

An important input into the theory of scattering are a class of second-order differential equations known as *Sturm-Liouville* problems. While these are a standard part of any course of mathematical methods for physics, I review here the crucial points. For more details consult your favorite mathematical methods text.

Appendix B

The three-dimensional harmonic oscillator

Consider the harmonic oscillator potential $V(r) = \frac{1}{2}m\omega^2 r^2$. Assume the usual factorization of the wavefunction in spherical coordinates,

$$\Psi_{nlm}(r,\theta,\phi) = \frac{u_{nl}(r)}{r} Y_{lm}(\theta,\phi). \tag{B.1}$$

This yields the radial Schrödinger equation

$$\left(-\frac{\hbar^2}{2m}\frac{d^2}{dr^2} + \frac{\hbar^2}{2m}\frac{l(l+1)}{r^2} + \frac{1}{2}m\omega^2 r^2 - E\right) u_{nl}(r) = 0. \tag{B.2}$$

Introducing the oscillator length

$$b = \sqrt{\frac{\hbar}{m\omega}} \tag{B.3}$$

and the dimensionless variables $y = r/b$ and $\epsilon = E/\hbar\omega$, we get the scaled equation

$$\left(-\frac{1}{2}\frac{d^2}{dy^2} + \frac{1}{2}\frac{l(l+1)}{y^2} + \frac{1}{2}y^2 - \epsilon\right) u(y) = 0. \tag{B.4}$$

As a first step, let

$$u(y) = y^{l+1} f(y). \tag{B.5}$$

This transforms the equation to

$$\left(-\frac{1}{2}\frac{d^2}{dy^2} - \frac{l+1}{y}\frac{d}{dy} + \frac{1}{2}y^2 - \epsilon\right) f(y) = 0. \tag{B.6}$$

As a next step, let $x = y^2$, so that

$$\frac{d}{dy} = \frac{dx}{dy}\frac{d}{dx} = 2\sqrt{x}\frac{d}{dx}, \quad \frac{d^2}{dy^2} = 4x\frac{d^2}{dx^2} + 2\frac{d}{dx}, \tag{B.7}$$

yielding

$$\left(-2x\frac{d^2}{dx^2} - (2l+3)\frac{d}{dx} + \frac{1}{2}x - \epsilon\right) f(x) = 0 \tag{B.8}$$

The final step is to take

$$f(x) = \exp(-x/2)p(x) \tag{B.9}$$

which leads to

$$\left(x\frac{d^2}{dx^2} + (l+3/2-x)\frac{d}{dx} - \frac{1}{4}(2l+3-2\epsilon)\right) p(x) = 0. \tag{B.10}$$

One can solve this by a power series, but the power series are just associated Laguerre polynomials.

B.1 Associated Laguerre polynomials

Part of the trickiness of associated Laguerre polynomials is that there are two different conventions for normalization. Let me start first with the Laguerre polynomial $L_n(x)$, which has the differential equation

$$\left(x\frac{d^2}{dx^2} + (1-x)\frac{d}{dx} + n\right) L_n(x) = 0. \tag{B.11}$$

The Rodrigues representation has two different normalizations. The one frequently used in quantum mechanics is

$$L_n(x) = \frac{e^x}{n!}\frac{d^n}{dx^n}\left(x^n e^{-x}\right) \tag{B.12}$$

which has normalization $L_n(0) = 1$; but another normalization found in some mathematical methods books is

$$L_n(x) = e^x\frac{d^n}{dx^n}\left(x^n e^{-x}\right) \tag{B.13}$$

which has normalization $L_n(0) = n!$.

This discussion carries over to the associated Laguerre polynomials, which have the differential equation

$$\left(x\frac{d^2}{dx^2} + (k+1-x)\frac{d}{dx} + n\right) L_n^k(x) = 0. \tag{B.14}$$

where k does not have to be an integer (but $k = 0$ gives us the regular Laguerre polynomial); the two Rodrigues representations are

$$L_n^k(x) = \frac{x^{-k}e^x}{n!}\frac{d^n}{dx^n}\left(x^{n+k}e^{-x}\right) \tag{B.15}$$

which has normalization $L_n^k(0) = \Gamma(n+k+1)/n!\Gamma(k+1)$.

(There is an alternate definition and normalization,

$$L_n^k(x) = x^{-k}e^x \frac{d^n}{dx^n}\left(x^{n+k}e^{-x}\right) \tag{B.16}$$

which has normalization $L_n^k(0) = \Gamma(n+k+1)/\Gamma(k+1)$, but in the notes that follow I will write the solutions in terms of the first normalization convention.)

The associated Laguerre polynomial is, as a series,

$$L_n^k(x) = \sum_{m=0}^{n} (-1)^m \frac{1}{m!} \frac{\Gamma(n+k+1)}{\Gamma(n-m+1)\Gamma(k+m+1)} x^m. \tag{B.17}$$

Note that the associated Laguerre polynomial can be written in terms of confluent hypergeometric series.

The normalization integral for the associated Laguerre polynomial is

$$\int_0^\infty e^{-x}x^{k+1}\left(L_n^k(x)\right)^2 dx = \frac{\Gamma(n+k+1)}{n!}. \tag{B.18}$$

B.1.1 Recursion relations

It's useful to have various recursion relations. For example, examining (B.17) one finds

$$L_{n-1}^{k+1}(x) = -\frac{d}{dx}L_n^k(x). \tag{B.19}$$

Other useful recursion relations are

$$xL_n^k(x) = (2n+k+1)L_n^k(x) - (n+k)L_{n-1}^k(x) - (n+1)L_{n+1}^k(x) \tag{B.20}$$

which can also be rewritten as

$$(n+1)L_{n+1}^k(x) = (2n+k+1-x)L_n^k(x) - (n+k)L_{n-1}^k(x). \tag{B.21}$$

There is also the derivative recursion

$$x\frac{d}{dx}L_n^k(x) = nL_n^k(x) - (n+k)L_{n-1}^k(k). \tag{B.22}$$

Alternately, one can use a generating function

$$\frac{\exp(-xz/(1-z))}{(1-z)^{k+1}} = \sum_{n=0}^{\infty} L_n^k(x)z^n \tag{B.23}$$

which leads to

$$\sum_{n=0}^{\infty} L_n^{k+1}(x)z^n = \frac{1}{1-z}\sum_{n=0}^{\infty} L_n^k(x)z^n \tag{B.24}$$

or the following recursion relations:

$$L_n^k(x) = L_n^{k+1} - L_{n-1}^{k+1}, \tag{B.25}$$

$$L_n^{k+1}(x) = \sum_{i=0}^{n} L_i^k(x). \tag{B.26}$$

B.2 Application to the 3D harmonic oscillator

Looking back at Eq. B.10, if we define $\epsilon = 2n+l+3/2$, then we get the associated Laguerre equation B.14 with $k = l + 1/2$. Then we get the special form

$$L_n^{l+1/2}(x) = \sum_{m=0}^{n} (-1)^m \frac{1}{m!} \frac{\Gamma(n+l+1+1/2)}{\Gamma(n-m+1)\Gamma(l+m+1+1/2)} x^m. \tag{B.27}$$

For this we use $\Gamma(j+1/2) = \sqrt{\pi}\frac{(2j-1)!!}{2^j}$ to get

$$L_n^{l+1/2}(x) = \sum_{m=0}^{n} (-1)^m \frac{1}{m!} \frac{(2n+2l+1)!!}{2^{n-m}(n-m)!(2m+2l+1)!!} x^m. \tag{B.28}$$

To get for arbitrary n, one should use the recursion (B.21), starting with

$$L_0^{l+1/2}(x) = 1, \tag{B.29}$$

$$L_1^{l+1/2}(x) = l + \frac{3}{2} - x, \tag{B.30}$$

and then recurse up to n.

Finally, the radial wavefunction is, up to a normalization

$$u_{nl}(r) = N_{nl}(r/b)^{l+1} \exp(-\frac{1}{2}(r/b)^2) L_n^{l+1/2}((r/b)^2) \tag{B.31}$$

This must be normalized by

$$\int_0^\infty |u_{nl}(r)|^2 dr = 1. \tag{B.32}$$

If we let $z = (r/b)^2$, then we have the normalization condition

$$\frac{1}{2} N_{nl}^2 b^3 \int_0^\infty e^{-z} z^{l+1/2} \left(L_n^{l+1/2}(z)\right)^2 dz = 1 \tag{B.33}$$

which, using the normalization integral (B.18) for the associated Laguerre polynomial, gives

$$N_{nl} = \sqrt{\frac{2n!}{b^3\Gamma(n+l+3/2)}}, \tag{B.34}$$

or, using the double-factorial,

$$N_{nl} = \sqrt{\frac{2^{n+l+2}n!}{b^3\sqrt{\pi}(2n+2l+1)!!}}, \tag{B.35}$$

How to validate wave functions. Whenever one writes a numerical routine to generate a function, one should validate it. Here is how I validated my person routines for radial harmonic oscillator wave functions:

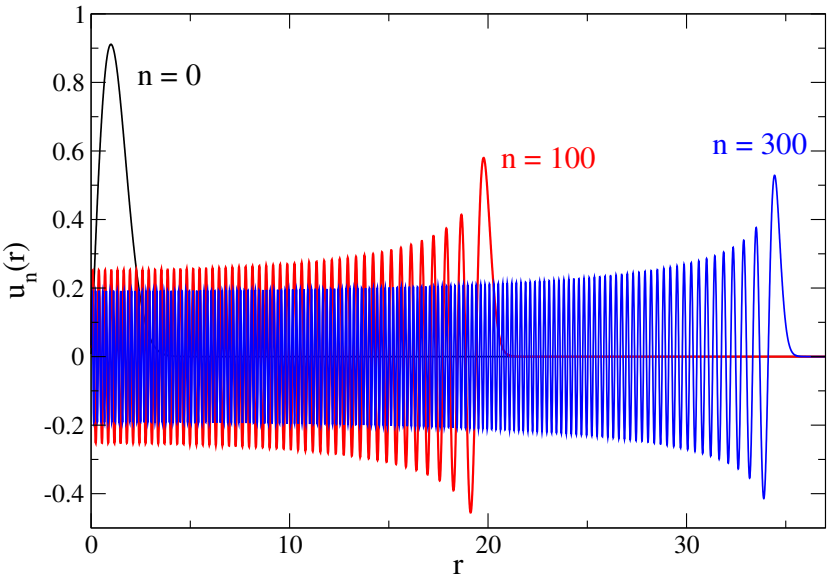

Figure B.1: Radial spherical harmonic oscillator wavefunctions $u_n(r)$ for $n = 0, 100, 300$, with length parameter $b = 1$.

• I wrote routines for generating the associated Laguerre polynomials using the series expansion (B.17) and the recursion (B.21), and then compared for relatively low ℓ and n.
• For general use, recursion should be more stable. To test further the full wave functions, as given by (B.31), you should use quadrature to check they satisfy the orthonormality condition,

$$\int_0^\infty u_{n'\ell}(r)\, u_{n\ell}(r)\, dr = \delta_{n'n}. \tag{B.36}$$

Such a test is also useful to make sure your numerical quadrature routines are well matched to your wave functions; if there are too few points or an inadequate range, (B.36) will be significantly violated.
• Finally, you should also test some of the matrix elements in the next section, such as

$$\langle n', \ell | r | n, \ell \rangle = \int_0^\infty u_{n'\ell}(r)\, r\, u_{n\ell}(r)\, dr. \tag{B.37}$$

That will aid you to have confidence both in the wave function and in the matrix elements.

B.3 Advanced calculation of matrix elements

While using the recursion (B.21) to get the Laguerre associated polynomial and then (B.31) to get the full radial wave function works, for large r/b and large n it

breaks down. This can be easily understood. If you look at Fig. B.1 (which just reproduces Fig. 5.2), you can see that for large n, the wave functions extend out to large r/b, roughly $2\sqrt{n}$. However the Gaussian term $\exp(-r^2/2b^2)$ in (B.31) will get very small, which in turn means the Laguerre associated polynomial must get correspondingly large. In practical computations this leads to errors or even `NaN` (not-a-number) flags.

To address this issue, I propose (but still have to test) a modified recursion. For some targeted n, define

$$\tilde{L}^k_m(x) \equiv \exp\left(-\frac{mx}{2n}\right) L^k_m(x) = z^m L^k_m(x), \tag{B.38}$$

where $z = \exp(-x/2n)$, which for large $x = (r/b)^2$ i is not as tiny as $\exp(-x/2)$ and therefore less problematic, so that

$$\tilde{L}^k_n(x) \equiv \exp\left(-\frac{x}{2}\right) L^k_n(x).$$

Then the recursion relation (B.21) becomes modified to

$$(m+1)\tilde{L}^k_{m+1}(x) = (2m+k+1-x)z\,\tilde{L}^k_m(x) - (m+k)z^2\,\tilde{L}^k_{m-1}(x). \tag{B.39}$$

I believe with this recursion the growth in $L^k_m(x)$ with m is compensated by multiplication by z, so that the final result is more tractable.

B.4 Matrix elements

I can use the recursion relations and definitions of the h.o. radial wavefunction to compute various matrix elements I need.

For example, one can derive that

$$rR_{nl} = \frac{N_{nl}}{N_{n,l+1}} R_{n,l+1} - \frac{N_{nl}}{N_{n-1,l+1}} R_{n-1,l+1}. \tag{B.40}$$

Then one easily gets the following:

$$\langle n, l+1|r|nl\rangle = \frac{N_{nl}}{N_{n,l+1}} = \sqrt{n+l+3/2}, \tag{B.41}$$

$$\langle n-1, l+1|r|nl\rangle = -\frac{N_{nl}}{N_{n-1,l+1}} = -\sqrt{n}. \tag{B.42}$$

Similarly, I need the matrix element

$$\left\langle n', l+1 \left| \frac{d}{dr} - \frac{l}{r} \right| n, l \right\rangle \tag{B.43}$$

Using the above one can show that

$$\left(\frac{d}{dr} - \frac{l}{r}\right) R_{nl} = -rR_{nl} - 2\frac{N_{nl}}{N_{n-1,l+1}} R_{n-1,l+1} \tag{B.44}$$

which yield

$$\left\langle n, l+1 \left| \frac{d}{dr} - \frac{l}{r} \right| n, l \right\rangle = -\sqrt{n+l+3/2}, \tag{B.45}$$

$$\left\langle n-1, l+1 \left| \frac{d}{dr} - \frac{l}{r} \right| n, l \right\rangle = -\sqrt{n} \tag{B.46}$$

Appendix C

Special functions

C.1 Spherical Bessel functions and how to compute them

$$j_\ell(x) = 2^\ell x^\ell \sum_{s=0}^{\infty} (-1)^s \frac{1}{s!(2s+2\ell+1)!} \left(\frac{x}{2}\right)^{2s} \tag{C.1}$$

$$= 2^\ell x^\ell \left[\frac{\ell!}{(2\ell)!} - \frac{(\ell+1)!}{(2\ell+3)!} \left(\frac{x}{2}\right)^2 + \frac{(\ell+2)!}{(2\ell+5)!} \left(\frac{x}{2}\right)^4 + \ldots \right] \tag{C.2}$$

and

$$n_\ell(x) = -\frac{1}{2^\ell x^{\ell+1}} \left[\sum_{s=0}^{\ell} \frac{(2\ell-2s)!}{s!(\ell-s)!} x^{2s} + (-1)^\ell \sum_{s=\ell+1}^{\infty} (-1)^s \frac{(s-\ell)!}{s!(2s-2\ell)!} x^{2\ell} \right] \tag{C.3}$$

$$= -\frac{(2\ell)!}{2^\ell \ell!} \frac{1}{x^{\ell+1}} + \ldots ... \tag{C.4}$$

We may have need of the recurrance relations

$$(2\ell+1)\frac{d}{dx} f_\ell(x) = \ell f_{\ell-1}(x) - (\ell+1) f_{\ell+1} \tag{C.5}$$

$$\frac{d}{dx} f_\ell(x) = -f_{\ell+1}(x) + \frac{\ell}{x} f_\ell(x) \tag{C.6}$$

$$f_{\ell-1}(x) + f_{\ell+1}(x) = \frac{2\ell+1}{x} f_\ell(x), \tag{C.7}$$

where f_ℓ is either the spherical Bessel or Neumann function. When we deal with the finite square well, we will also have need for the following (you should

derive from the above):

$$\frac{d}{dx}\left(xf_\ell(x)\right) = \frac{\ell+1}{x}xf_\ell(x) - xf_{\ell+1}(x) \tag{C.8}$$

$$\frac{d}{dx}\left(xf_\ell(x)\right) = \frac{1}{2\ell+1}\left((\ell+1)xf_{\ell-1}(x) - \ell xf_{\ell+1}(x)\right) \tag{C.9}$$

C.2 Computing

To compute the spherical Bessel functions, we use the recurrance relation (C.7). The problem is, this recurrance is stable upwards, that is for increasing n, only for the spherical Neumann functions. What this means is that, for arbitrary x, one can start with known spherical Neumann functions

$$n_0(x) = -\frac{\cos x}{x}, n_1(x) = -\frac{\cos x}{x^2} - \frac{\sin x}{x}, \tag{C.10}$$

and applying (C.7) can one get $n_\ell(x)$ for $\ell = 2, 3, 4, \ldots$. If, however, one applies the upward recursion to spherical Bessel functions, from numerical noise will grow a 'contamination' of Neumann functions.

Instead, I propose an alternate approach. We see that we can write both spherical Bessel and spherical Neumann functions in the form

$$y_\ell(x) = \frac{A_\ell(x)\sin x + B_\ell(x)\cos x}{x^{\ell+1}} \tag{C.11}$$

where $A_\ell(x)$, $B_\ell(x)$ are polynomials; from (C.7) one easily gets the polynomial recursion relation

$$A_\ell(x) = (2\ell-1)A_{\ell-1}(x) - x^2A_{\ell-2}(x), \tag{C.12}$$

with the same for $B_\ell(x)$. To start the recursion, for spherical Bessel functions,

$$A_0 = 1, \quad A_1 = 1, \quad , B_0 = 0, \quad B_1 = -x,$$

and for spherical Neumann functions,

$$A_0 = 0, \quad A_1 = -x, \quad B_0 = -1, \quad B_1 = -1.$$

The stability of this method needs to be investigated, but for modest ℓ I am pretty sure it should be relatively stable. My tests against online calculators show agreement to ten decimal places for a fairly wide range of values, so it seems to be stable.

The beauty is one can simplify this even further; by looking at the starting polynomials, we can see

$$j_\ell(x) = \frac{A_\ell(x)\sin x + B_\ell(x)\cos(x)}{x^{\ell+1}}, \tag{C.13}$$

$$n_\ell(x) = \frac{B_\ell(x)\sin(x) - A_\ell(x)\cos(x)}{x^{\ell+1}}, \tag{C.14}$$

if we use the A, B for spherical Bessel functions. Probably someone noticed this a long time ago....

Appendix D

Cauchy's residue theorem and evaluation of integrals

This appendix is not a substitute for a proper course or monograph on complex analysis.

Cauchy's residue theorem states that, if one integrates along a counterclockwise path that encloses a pole at z_0 in the complex plane, then

$$\oint \frac{f(z)}{z - z_0}\, dz = 2\pi i f(z_0). \tag{D.1}$$

This can be used to evalulate some real integrals. As an example, consider

$$I = \int_0^\infty \frac{1}{x^2} \sin ax \sin bx\, dx$$

Let's assume $a \geq b > 0$, and also a, b both real. The integrand is even, so we go along the entire real axis:

$$I = \frac{1}{2} \int_{-\infty}^\infty \frac{1}{x^2} \sin ax \sin bx\, dx \tag{D.2}$$

Now using a trig identity, and substituting in $A = a - b$ and $B = a + b$, both positive by assumption.

$$= \frac{1}{4} \int_{-\infty}^\infty \frac{1}{x^2} \left(\cos Ax - \cos Bx\right)\, dx \tag{D.3}$$

$$= \frac{1}{8} \int_{-\infty}^\infty \frac{1}{x^2} \left(e^{iAx} + e^{-iAx} - e^{iBx} - e^{-iBx}\right)\, dx. \tag{D.4}$$

Now, in order to get ready for applying Cauchy's theorem, we write this as (with a little rearrangement)

$$= \lim_{\epsilon \to 0^+} \frac{1}{8} \int_{-\infty}^\infty \frac{1}{x^2 + \epsilon^2} \left(e^{iAx} - e^{iBx} + e^{-iAx} - e^{-iBx}\right)\, dx. \tag{D.5}$$

The superscript $^+$ denotes we keep the infinitesmal quantity ϵ positive. We rewrite

$$\frac{1}{x^2+\epsilon^2} = \frac{1}{2i\epsilon}\left[\frac{1}{x-i\epsilon} - \frac{1}{x+i\epsilon}\right] \tag{D.6}$$

The first term has a pole at $z = i\epsilon$ which is in the *upper half complex plane*, that is, that part with $\Im z > 0$, because we have assume $\epsilon \geq 0$. The second term has a pole at $z = -i\epsilon$, which is the *lower half complex plane*, with $\Im z < 0$.

Now we want to imagine taking a very, very large closed path in the complex plane. Part of the path will be along the real axis, but then we will sweep over and around either the upper half plane, or the lower half plane. Now because A, B are real and positive, then e^{iAz} and $e^{iBz} \to 0$ for $\Im z$ large and positive, that is, in the upper half-plane. So if we take our path along the real axis, and then loop over the upper half-plane, those terms will vanish except along the real axis. [Note: some day I will add a figure illustrating this.]

So we write:

$$\frac{1}{8}\int_{-\infty}^{\infty} \frac{1}{x^2+\epsilon^2}\left(e^{iAx} - e^{iBx}\right)\,dx \tag{D.7}$$

$$= \frac{1}{8}\oint \frac{1}{2i\epsilon}\left[\frac{1}{z-i\epsilon} - \frac{1}{z+i\epsilon}\right]\left(e^{iAz} - e^{iBz}\right)\,dz \tag{D.8}$$

where the path is in the upper-half plane. Of the two poles, only the first one is in the upper half plane, hence, finally applying Cauchy's residue theorem, these terms become

$$\frac{1}{8}\frac{1}{2i\epsilon}2\pi i\left(e^{iA(i\epsilon)} - e^{iB(i\epsilon)}\right) = \frac{\pi}{8\epsilon}\left(e^{-A\epsilon} - e^{-B\epsilon}\right). \tag{D.9}$$

Taking the limit $\epsilon \to 0^+$, we get

$$\frac{\pi}{8}(B-A) = \frac{\pi b}{4}. \tag{D.10}$$

I leave it as a healthy exercise for the reader to show the remaining terms yield the same value; the only wrinkle is that the path in the lower half plane is *clockwise*, which gives us a negative sign in Cauchy's residue theorem. Adding together the final result is

$$I = \frac{\pi b}{2}$$

Appendix E

Orthogonal polynomials

In physics in general, and in quantum mechanics in particular, we are familiar with families of orthogonal functions and polynomials: Laguerre, Legendre, Hermite, and other polynomials and associated functions are useful tools. But the general theory of orthogonal polynomials is an astonishingly rich and deep field, with applications not only to scattering but to other topics as diverse as random matrices. Here I will only barely touch upon them.

If you have taken a typical course on quantum mechanics–and you ought to have, in order to be able to use this text–you are familiar with the idea of linear vector spaces of functions. The basic idea is that one can consider a space of function, where one can expand any function $f(x)$ in the space in a set of basis functions $\{\phi_n(x)\}$,

$$f(x) = \sum_n c_n \phi_n(x), \tag{E.1}$$

and where some definition of an inner product between functions allows you to find the coefficients c_n. One of the most widespread examples are Fourier series. We call such a function space a Hilbert space.

Orthogonal polynomials are an example of this. Define an inner product with a *weight function* $w(x)$:

$$(f, g) \equiv \int_a^b f^*(x) w(x) g(x)\, dx \tag{E.2}$$

Despite the complex conjugate, we will general restrict ourselves to real-valued functions in this discussion. In order for this to be a well-constructed inner product, the weight function should be positive-definite.

Now that we have an inner product, we have a clear idea of when two functions are "orthogonal" to each other:

$$(f, g) \equiv \int_a^b f^*(x) w(x) g(x)\, dx = 0.$$

Now consider that we have a set of polynomials, $p_n(x)$, each labeled by the order, so that

$$p_n(x) = \sum_{j=0}^{n} p_j^{(n)} x^j. \tag{E.3}$$

For now let's assume the coefficients $p_j^{(n)}$ are real, though this is not required. We want these polynomials to be orthogonal to each other, though not necessarily normalized, that is,

$$\int_a^b w(x) p_m(x) p_n(x)\, dx = N_n \delta_{m,n}. \tag{E.4}$$

We can characterize this through the *moments* of the inner product, that is,

$$\mu_k = \int_a^b x^k w(x)\, dx, \tag{E.5}$$

and, in fact, one of the many applications of orthogonal polynomials is to a topic called the *classical moment problem.* Then the orthogonality condition becomes

$$\sum_{j=0}^{m} \sum_{k=0}^{n} p_j^{(m)} p_k^{(n)} \mu_{j+k} = N_m \delta_{m,n}. \tag{E.6}$$

One can easily construct the polynomials one by one. Let's suppose we've constructed polynomials up through order $n-1$, so that we know $p_j^{(m)}$ for $m < n$. Then the conditions for the coefficients of $p_n(x)$ are

$$\sum_{j=0}^{m} \sum_{k=0}^{n} p_j^{(m)} p_k^{(n)} \mu_{j+k} = 0. \tag{E.7}$$

One way to think about this is to think of the coefficients as a vector, $\vec{p}_m$, and construct from the moments a positive-definite matrix

$$M_{j,k} = \mu_{j+k}; \tag{E.8}$$

then one is orthogonalizing each new vector against the old ones by

$$\vec{p}_m^{\,T} \cdot \mathbf{M} \cdot \vec{p}_n = 0 \tag{E.9}$$

for $m \neq n$, which leads to a Gram-Schmidt-like orthogonalization process. One difference is that we do not require normalization; this is simply a choice that is historical.

While such a process is fairly intuitive, at least to someone who has been exposed to linear functions spaces in quantum mechanics or some mathematical methods course, less obvious is the recursion relation, which says that, given some value of x and knowing the values of $p_{n-1}(x)$ and $p_{n-2}(x)$ we can calculate $p_n(x)$.

It should be self-evident that any polynomial $f(x)$ of order k can be written as a linear combination of polynomials $p_0(x)$ through $p_k(x)$,

$$f(x) = \sum_{m=0}^{k} c_m p_m(x), \tag{E.10}$$

and in fact we can find the expansion coefficients through our inner product:

$$c_m = \frac{(f(x), p_m(x))}{(p_m(x), p_m(x))^{1/2}} = \frac{1}{\sqrt{N_m}} \int_a^b w(x) f(x) p_m(x)\, dx, \tag{E.11}$$

where we've put in the explicit normalization of $p_m(x)$.

We're now going to use this in two different ways. The first is to prove a lemma, which is that not only is any orthogonal polynomial $p_n(x)$ orthogonal to all $p_m(x)$ for $m \neq n$, it is also orthogonal to *any* polynomial of order $m < n$. This sounds surprising at first, but consider a polynomial $g(x)$ of order m. It can be expanded as usual:

$$g(x) = \sum_{j=0}^{m} d_j p_j(x), \tag{E.12}$$

but $p_n(x)$ with $n > m$ is orthogonal to each term in this expansion and hence is orthogonal to $g(x)$.

Now let's consider $p_n(x)$. To get the term proportional to x^n, we multiply p_{n-1} by x, that is, there should be some coefficient a_n such that

$$p_n(x) - a_n x p_{n-1}(x) \tag{E.13}$$

is a polynomial of order $n-1$ (because we've subtracted off the x^n part). Thus we know

$$p_n(x) = a_n x p_{n-1}(x) + \sum_{m=0}^{n-1} c_m p_m(x). \tag{E.14}$$

We can find the coeffcients c_m by the above procedure:

$$\begin{aligned} c_m &= N_m^{-1/2} \int_a^b w(x) \left(p_n(x) - a_n x p_{n-1}(x)\right) p_m(x)\, dx \\ &= -a_n N_m^{-1/2} \int_a^b w(x) p_{n-1}(x)\, x p_m(x)\, dx, \end{aligned} \tag{E.15}$$

because by definition $p_n(x)$ and $p_m(x)$ are orthogonal for $m < n$. Furthermore, $x p_m(x)$ is a polynomial of order $m+1$, hence by our lemma above it is orthogonal to $p_{n-1}(x)$ for any $m < n-2$. Thus we can write

$$p_n(x) = a_n x p_{n-1}(x) + b_n p_{n-1}(x) + c_n p_{n-2}(x). \tag{E.16}$$

This three-term recursion relation is what ties orthogonal polynomials to the J-matrix method of scattering, as well as other topics such as the Lanczos algorithm for diagonalization, both of which are couched in terms of tridiagonal matrices.